PNC TN9410 92-018

Study of thermohydraulic behavior within the fuel bundle under a loss of flow condition

January, 1992

OARAI ENGINEERING CENTER
POWER REACTOR AND NUCLEAR FUEL DEVELOPEMENT CORPORATION

複製又はこの資料の入手については，下記にお問い合わせください。
〒311-13　茨城県東茨城郡大洗町成田町4002
動力炉・核燃料開発事業団
大洗工学センター　システム開発推進部・技術管理室

Enquires about copyright and reproduction should be addressed to: Technology Management Section O-arai Engineering Center, Power Reactor and Nuclear Fuel Development Corporation 4002 Narita-cho, O-arai-machi, Higashi-Ibaraki, Ibaraki-ken, 311-13, Japan

動力炉・核燃料開発事業団（Power Reactor and Nuclear Fuel Development Corporation）

PNC TN9410 92-018
January, 1992

Study of thermohydraulic behavior within the fuel bundle under a loss of flow condition.

Muhammad Enamul Kabir* and
Hiroki Hayafune**.

Abstract

This report describes the result of the analysis of unprotected Loss of Flow (LOF) transient experiment conducted at the PLANt Dynamics Test Loop (PLANDTL) experimental facility by Super System Code (SSC) and SubAssembly Boiling EvolutioN Analysis (SABENA) code. This report also describes the effect of the modification we made in SSC with the recent void fraction and two-phase friction multiplier models during the analysis of the experiment. After the analysis, it was found that the two-fluid two-phase flow model of SABENA 1-D is better than the homogeneous model of SSC in predicting the thermohydraulic behavior within the simulated fuel bundle test section of the PLANDTL facility in case of high quality sodium boiling experiment. Moreover, it was also revealed that the two-fluid one dimensional model is not accurate enough in predicting the onset of boiling and axial evolution of boiling region inside the heated channel.

---

*ROMU, Atomic Energy Research Establishment, Bangladesh Atomic Energy Commission, P.O.Box- 3787, Dhaka, Bangladesh.

** Reactor Engineering Section, Safety Engineering Division, OEC, PNC.

Content

List of Figures

1. Introduction :

An accurate prediction of transient two-phase flow is essential to safety analysis of nuclear reactors under off-normal and accidental condition. In general the ability to predict these thermohydraulic phenomena of two-phase flow depends on the availability of mathematical model and experimental correlations. The fluid flow and heat transfer encountered in reactor safety analysis are often very complex due to reactor geometries and occurrence of transient two-phase flow. Various computer programmes have been developed for analysis of transient two-phase flow for liquid metal cooled Fast breeder reactor (LMFBR) and different solution techniques were used for the analysis. In order to verify the accuracy of these computer codes in predicting the off normal and accidental situation, both large and small scale experiments are simulated by these computer codes.

As already mentioned before, We have to study the transient sodium boiling experiment conducted at the plant dynamics test loop experimental facility of the Reactor Engineering Section of OEC,PNC by two different computer codes : i) Super System Code (SSC) and ii) Subassembly Boiling EvolutioN Analysis code.(SABENA). It is interesting to note that in analyzing the transient condition SSC employes the homogeneous flow model while SABENA employes the two-fluid separated flow model. So this study will provide me with the the opportunity to verify the analytical capabilities of these code in analyzing the low flow transient condition.

2.PLANt Dynamics Test Loop (PLANDTL) experimental facility :

2.1. Introduction :

The PLANt Dynamics Test Loop (PLANDTL) experimental facility was developed at the Reactor Engineering Section of OEC, PNC. The construction of this test facility was completed in September, 1987 and since then various thermohydraulic experiment were carried out in this facility with particular emphasize on Monju (demonstration fast breeder reactor of PNC) FBR's Loss Of Piping Integrity (LOPI) condition simulation. Figure : 2.1 shows a schematic view of the PLANDTL facility. PLANDTL has the following characteristics point:

i) it has the primary and secondary loop as well as the reactor core simulator section which made it possible to conduct thermal transient experiments including examination of typical plant system dynamics

ii) the core simulator consists of two parallel channel which allows the analysis of the effect of the core and plenum thermal transient hydraulic interaction during transient experiment due to difference between two channel condition.

iii) it has the capability of controlling the flow rate and bundle pin power using the computer system thus enabling the conduct of transient sodium boiling experiment under wide parameter combination.

iv) the plant control by the computer system enables the carry out of the plant dynamics experiment taking into account the negative and positive reactivity feedback effects of a reactor system by modulating the pin power upon request of calculational model of reactivity feedback.

A view of the 37 fuel pin bundle test section is shown in figure: 2.2 Test section dimension is shown in figure 2.3.

There were many sodium boiling experiment carried out in the PLANDTL experimental facility and out of them I have analyzed only the unprotected loss of flow (LOF) experiment no : 15057.

2.2 Outline of the LOF- 15057 experiment :

Loss of flow experiment no. 15057 was carried out in the PLANDTL experimental facility to investigate the sodium boiling behavior inside the test section in case of unprotected loss of flow accident. In this experiment of a hypothetical accident, a simultaneous failure of primary pumps and reactor shutdown system is assumed. In this particular test only one test channel was put in to operation . The test section geometry is summarized in table 1 .

The 37 pin heater section were installed in hexagonal inconel tube of 10mm thickness and the gap between the peripheral pins and the duct wall was about 1.5mm. Thermal insulation on the outer wall of the hexagonal tube minimizes heat loss through the duct wall.

The heater pin view is shown in figure : 2.4. The pin power profile is chopped cosine distribution and the ratio of average to maximum flux is 1 : 1.204.

The axial power profile of the heater pin is expressed by the following equation :

$$Q(x) = Q_{max} (0.9929704 \cos (0.0223841 (x - 46.5)) + 0.007079315)$$

$$Q_{max} = Q_{avg.} \times 1.204$$

$$Q_{avg.} = \text{total power} / (\pi \times 0.0065 \times 93 \times 37)$$

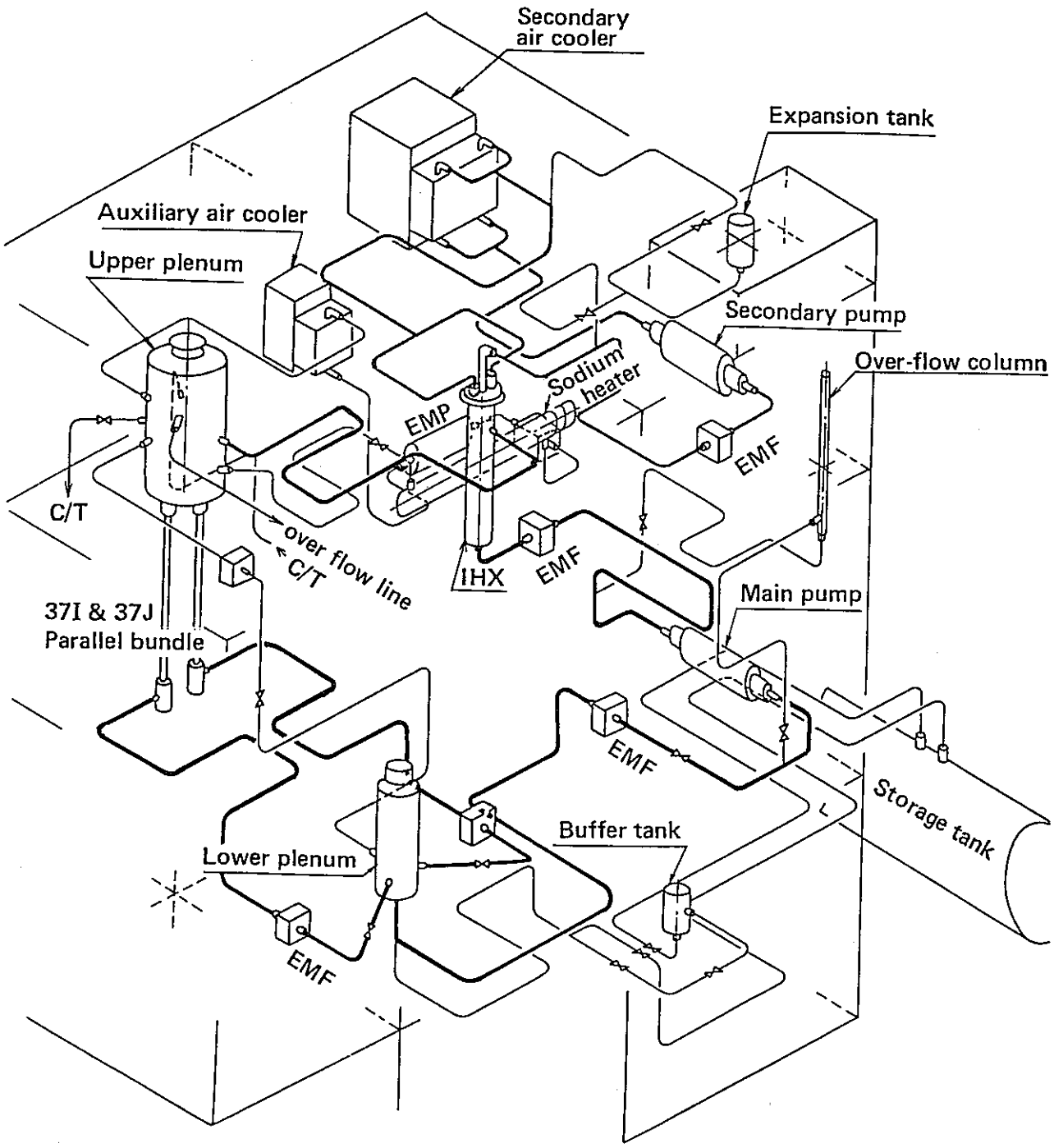

Figure 2.1 Schematic view of the PLANDTL facility.

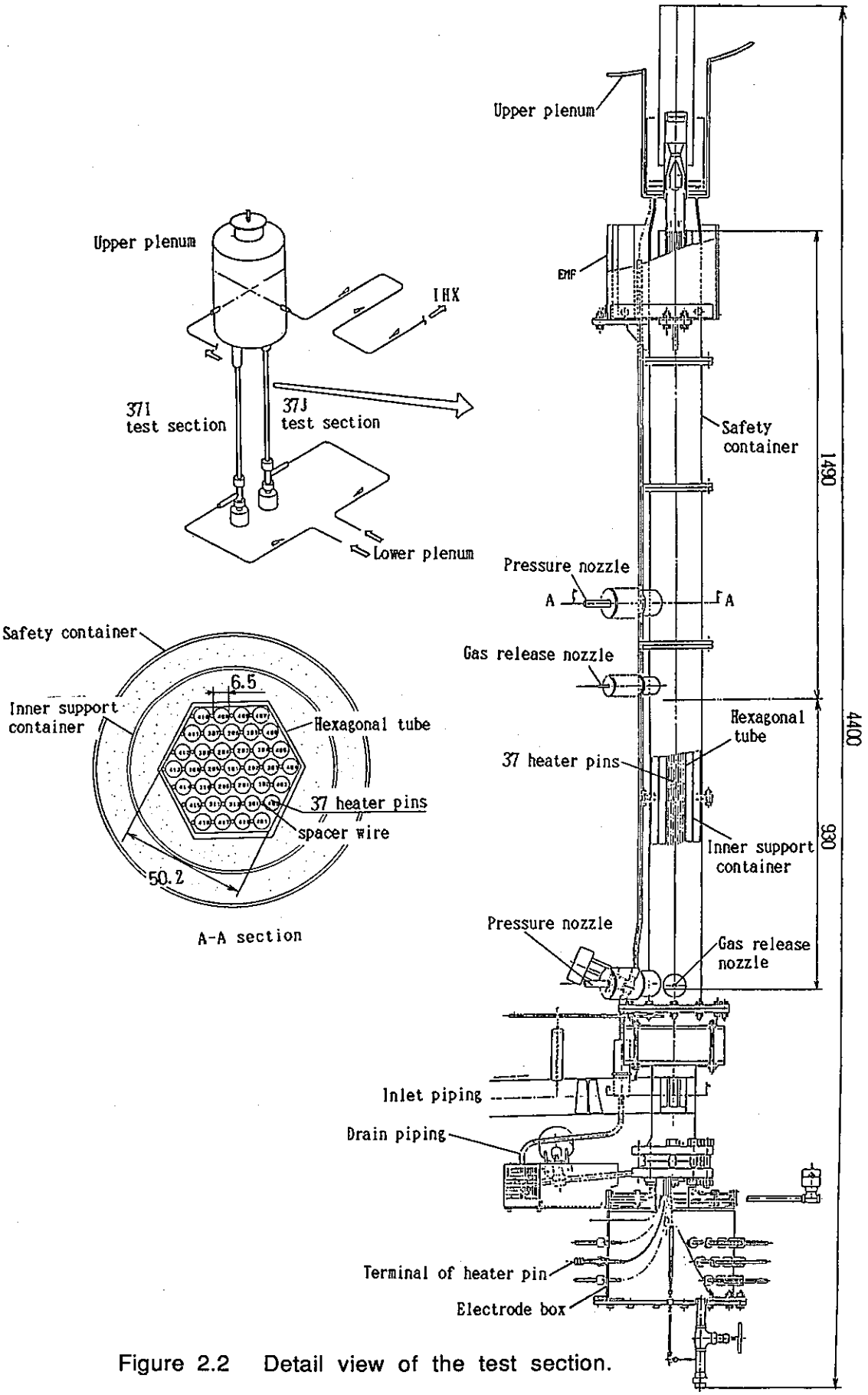

Figure 2.2 Detail view of the test section.

Test section dimension

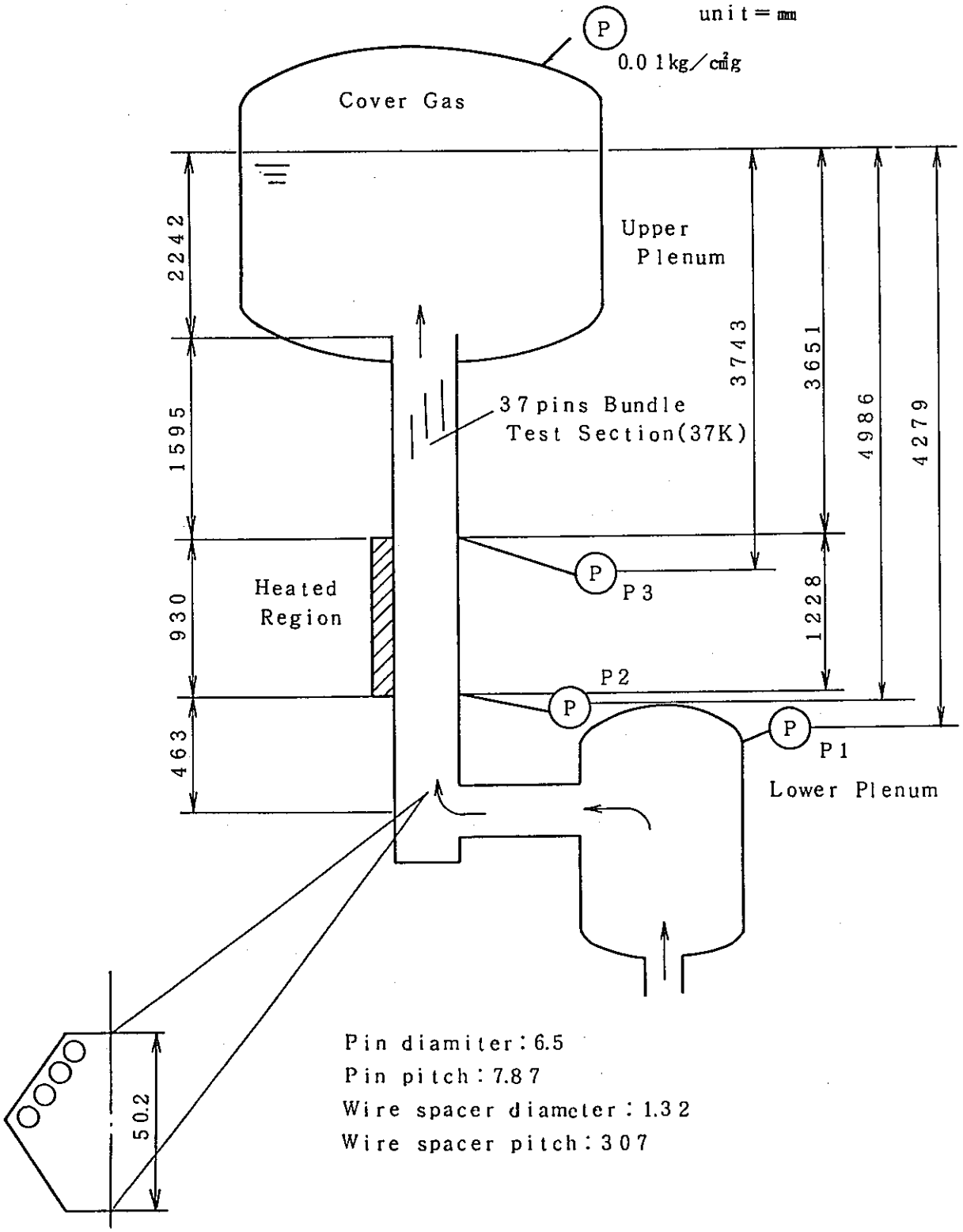

Figure 2.3 Test section dimension of the PLANDTL facility.

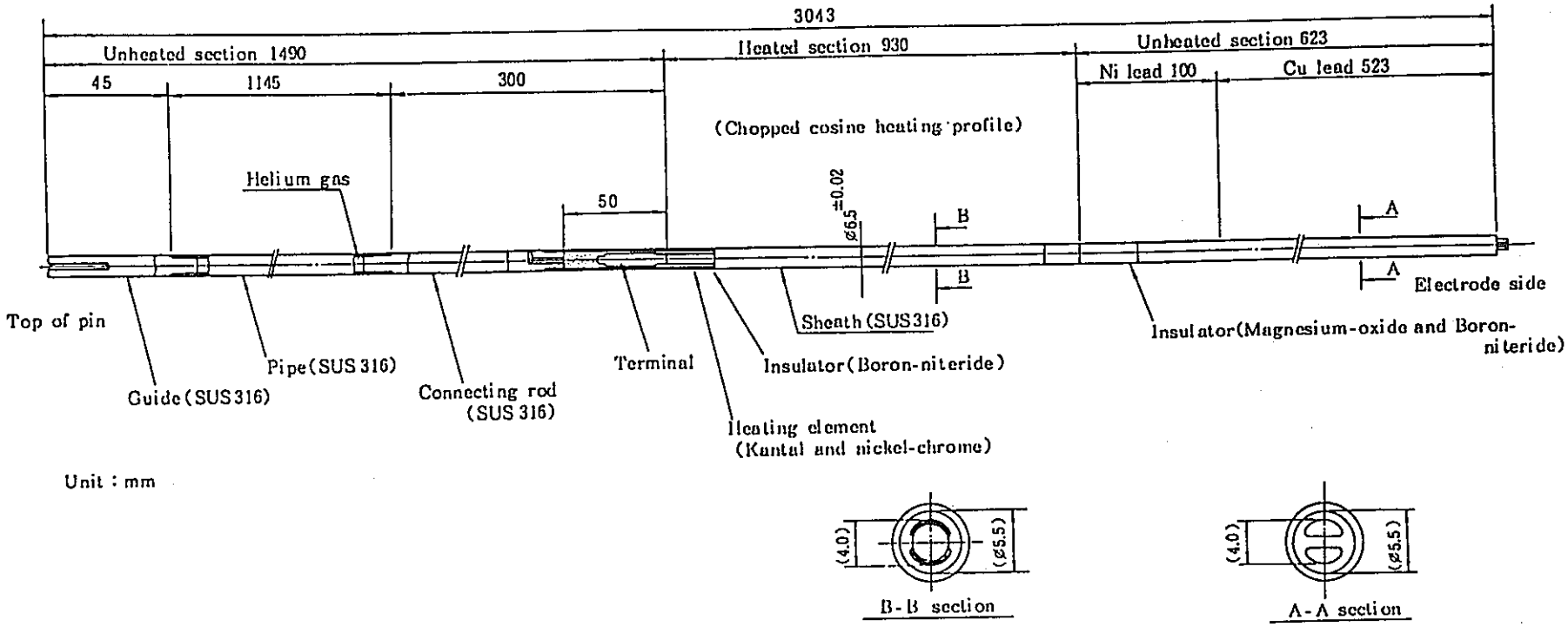

Figure 2.4 Heater pin Specification.

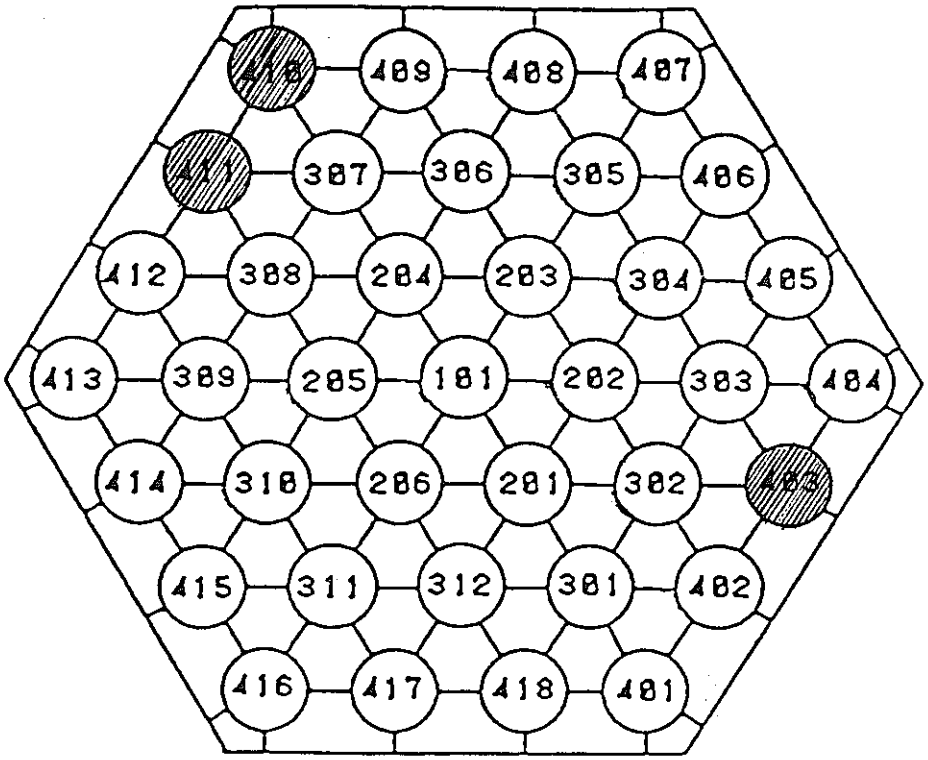

Figure 2.5 Location of unheated pin in the bundle.

Although there were 37 heater pin inside the test section but during LOF 15057 experiment 3 pins remained unheated as those pins were damaged during earlier test.

Figure : 2.5 shows the x-sectional view of the heater pin bundle and the location of the unheated pins inside the bundle.

The initial steady state test condition are : inlet sodium temperature is 398.8 deg C, cover gas pressure is 0.01 kg/cm^2, total power is100kW, inlet sodium flow rate is 0.275 kg/sec. This transient experiment was conducted by flow coast down method i,e, after the initial steady state had been reached the pump was switched off and the flow decreased according to predetermined characteristics. Sodium flow rate measured at the inlet of the test section is shown in figure : 2.6. Flow velocity was decreased from a maximum of 0.3407m/s to 0.001m/s within 6.5 second after the initiation of the transient. Due to the flow coast down, the temperature inside the bundle increased and after some time boiling of sodium started. This experiment was conducted for 180 seconds after the start of the transient and during this period test section power was kept at a constant 100KW level. Figure : 2.7 shows the test section power time history curve. During the transient ,the upper plenum cover gas remained constant as shown in figure : 2.8. During the conduct of the experiment, no dryout of the channel occured.

2.3. Analysis of experimental result :

In order to get information on the evolution of boiling and its axial and radial progression inside the test section, the entire test section was equipped with a large number of temperature measuring thermocouple at different axial location. A total of 166 thermocouples were installed at 51 axial position of the test section. Figure : 2.9 shows the axial positions where the thermocouples were placed. Detail distribution of the the thermocouples at 4 particular elevation of the test section is also shown in that figure. As shown in that figure, section BJ (Center of the heated section) and section BS (top of the heated section) were provided with maximum number of thermocouples and from the out

of those thermocouples, the radial temperature distribution information at those location throughout the experiment was available.

2.3.1. Single phase temperature distribution just before boiling inception :

The single phase axial temperature profile at the center of the test section just before the inception of boiling and radial temperature distribution at the top of the heated section (section BS) at the start of the transient experiment and just before the onset of boiling is shown in figure : 2.10 and figure : 2.11 respectively. The single phase temperature distribution especially that prevailed just before boiling inception is very important because the dynamics of expansion of sodium boiling region both in axial and radial direction depend on those profile.

From the axial temperature distribution curve for the central region of the test section, we find that there was a steep rise of temperature upto very near to the top of the heated section and then a steep decrease of temperature in the downstream section and at some position of the upper unheated part temperature reached to a almost constant level.

Since there were three unheated pins inside the fuel pin bundle, this affected the radial temperature distribution considerably. To get some idea about the effect of these unheated pins on the radial temperature, we have plotted the radial temperature profile from different edge to edge (through the center) of the hexagonal wrapper tube and from the curve we find that there was steep temperature gradient at those regions where the unheated pin were located compared with the other regions of the section. Moreover, we also find that the difference in temperature between the central region and the peripheral unheated pin region increased much more compared to the the other region of this section with the elapse of transient time. So, when the temperature of the central region reached the saturation level , at that time the temperature at the peripheral unheated pin region was about 200 deg.C below the saturation level. This steep radial temperature profile influenced

greatly the radial expansion of boiling region.

2.3.2. Sodium boiling behavior inside the test channel :

There were no void measuring devices inside the test section. From the temperature data generated by the thermocouples during the conduct of the transient experiment we find that temperature of sodium reached the saturation temperature at about 21 second near the top of the heated section as is shown by the axial temperature distribution curve of the central region of the test channel. At the top of the heated section boiling started at about 25.3 second of the transient time at the center of the bundle. As we know, after the inception of boiling, boiling region grew spatially, i.e. three dimensionally preferably within regions with flat temperature gradient. This fact is revealed from the temperature mapping curve for the BS section starting from beginning of transient to 40th. second of transient as shown from figure :2.12. From those plots we find that because of the nonuniform radial temperature distribution due to the presence of 3 unheated heater pins, boiling region after its inception grew eccentrically towards less steeper temperature gradient region. The expansion of boiling region towards the steeper temperature gradient region did not take place simultaneously due to the condensation of the vapor by the comparative subcooled sodium of those region. The condensation of vapor in those region gradually increased the temperature and at about 35th. second of transient, boiling region reached near the edge of the hexagonal wrapper tube in all side. So, due to the nonuniformity of the radial temperature distribution, it takes about 10 second to reach the boiling region near the periphery of the channel. After the boiling region reached the test section wall, then only axial growth of the region is the only possibility because now condensation areas in radial direction were strongly reduced and vapor flow changed into axial direction.

To get some idea about the axial expansion of the voided region we have plotted the transient time vs. the axial void region curve for the central region and the peripheral region as shown in figure : 2.13. As we have already mentioned that there were no void measuring devices in side the test channel, so we actually got the axial void progression curve by plotting the saturation temperature data for the central and peripheral region. From the axial void progression curve for the central region we find that the void region after its

inception near the center of the heated section grew slowly towards both upstream and downstream region of the heated section of the test channel until about 35th second of the transient. During this period the void progression is mostly radial due to the very low sodium flow velocity inside the channel. At around 35 second boiling front reached towards the wall of the channel (as discussed earlier) and then it started to move towards the unheated downstream section more rapidly as shown in the figure. From the peripheral void progression curve, we find that the progression is much faster towards the downstream unheated section. The reason for this behavior is in agreement with our earlier discussion that after the void region reached the wall of the subchannel it can move only towards axial direction. Since the location (distance from center and its position) of the thermocouples in different axial planes are not the same, so some point of the peripheral void progression curve is found outside the central channel curve which is quiet contradictory.

During the entire transient period, dryout of the channel did not occur. This is due to the fact that the even after the boiling region reached the wall of the test channel, there were always a thin layer of liquid film over the heater pin From the temperature vs transient time curve (figure :4.4) for different radial position of the section BS,.we find that although at some point of the experiment there were temperature spikes due to temporary dry out of the channel but the temperature returned back to the saturation temperature level by the rewetting of the dried out area by the deposition of liquid droplet which were entrained by the high velocity vapor

Table 1: Test section geometry

Item	
Number of pins	37
Diameter of pin	6.5 mm
Pin pitch	7.87 mm
Total length of pins	2988 mm
Length of unheated entrance region	398 mm
Length of the heated region	930 mm
Length of unheated downstream region	1490 mm
Material of clad	SAS316
Thickness of clad	0.47 mm
Diameter of spacer wire	1.32 mm
Wrapping pitch of spacer wire	307 mm
Flow area	921.4 mm
Equivalent Hydraulic diameter	3.4013 mm
Inner flat to flat distance of wrapper tube	50.4 mm
Thickness of wrapper tube	10 mm
Material of wrapper tube	inconel
Gap between outer pin surface and wrapper tube	1.5 mm

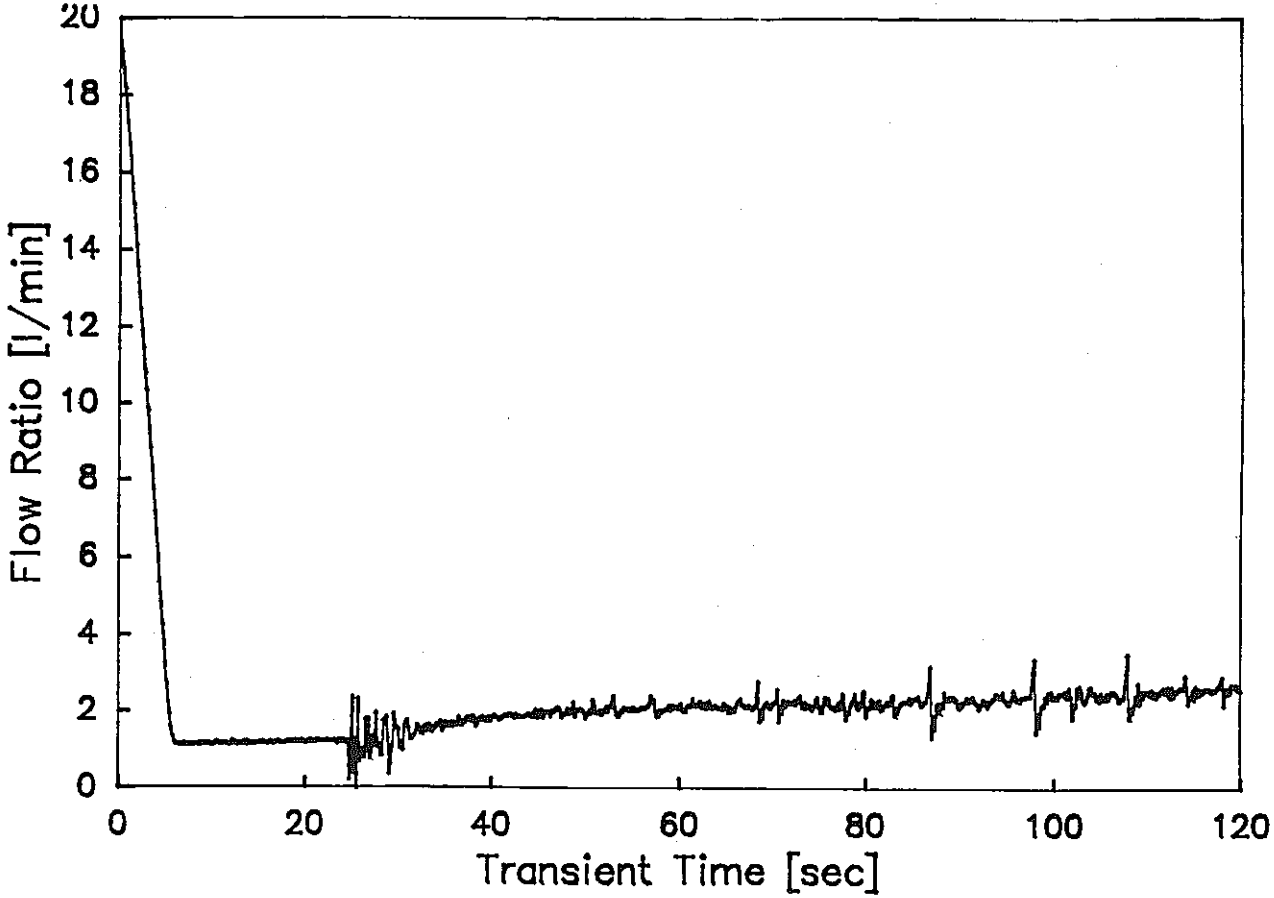

Figure 2.6 Sodium inlet flow rate during transient.

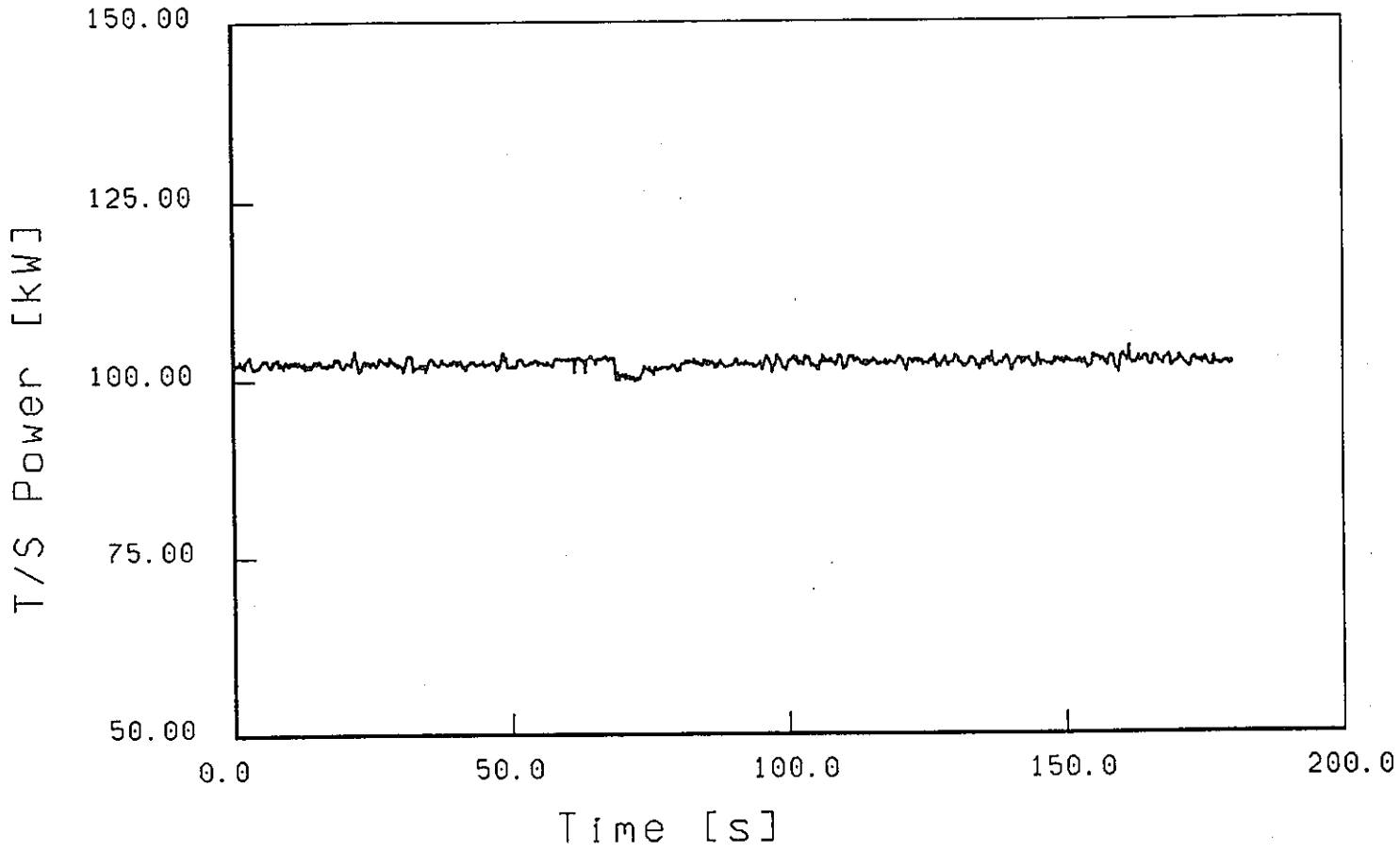

Figure 2.7 Test section power during transient.

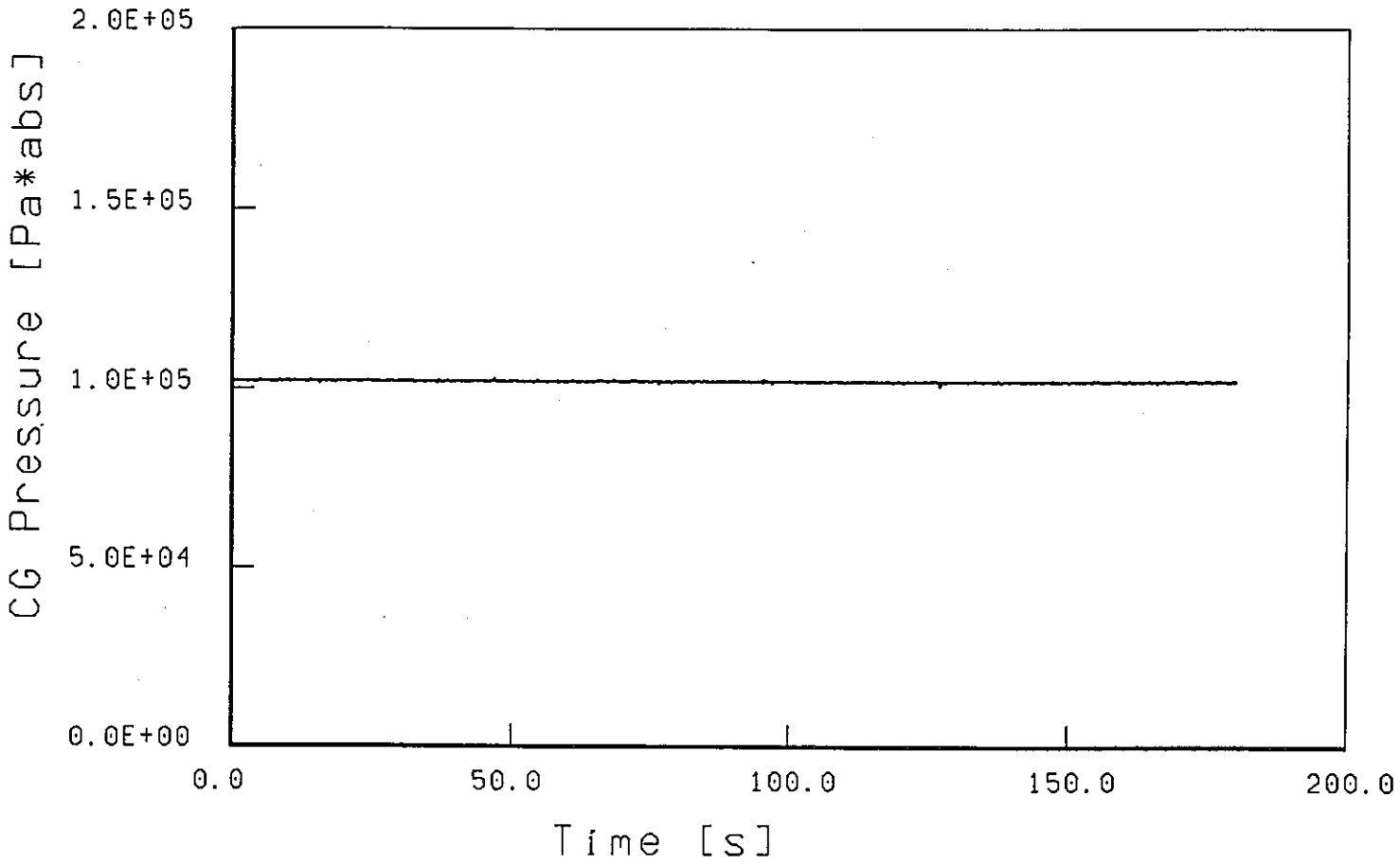

Figure 2.8 Cover gas pressure during transient.

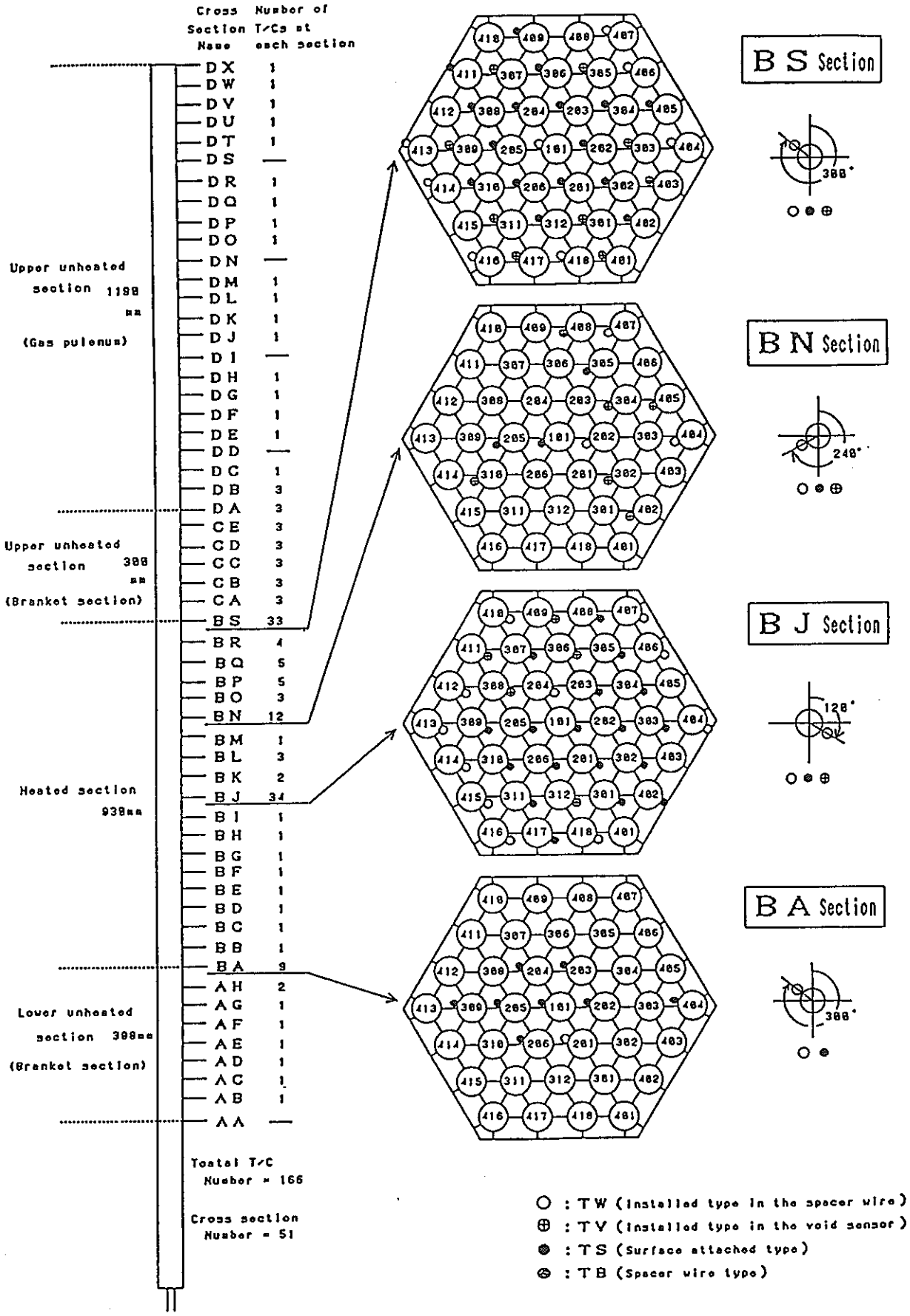

Figure 2.9 Location of thermocouple in the bundle.

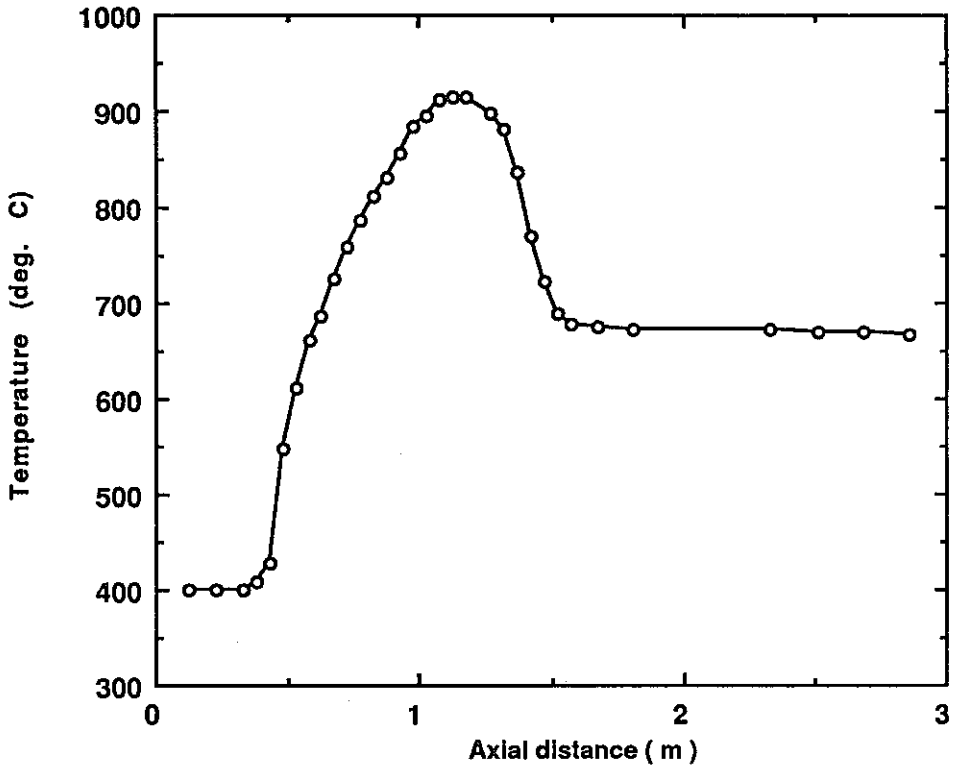

Figure 2.10 Axial temperature distribution before boiling. (Central region)

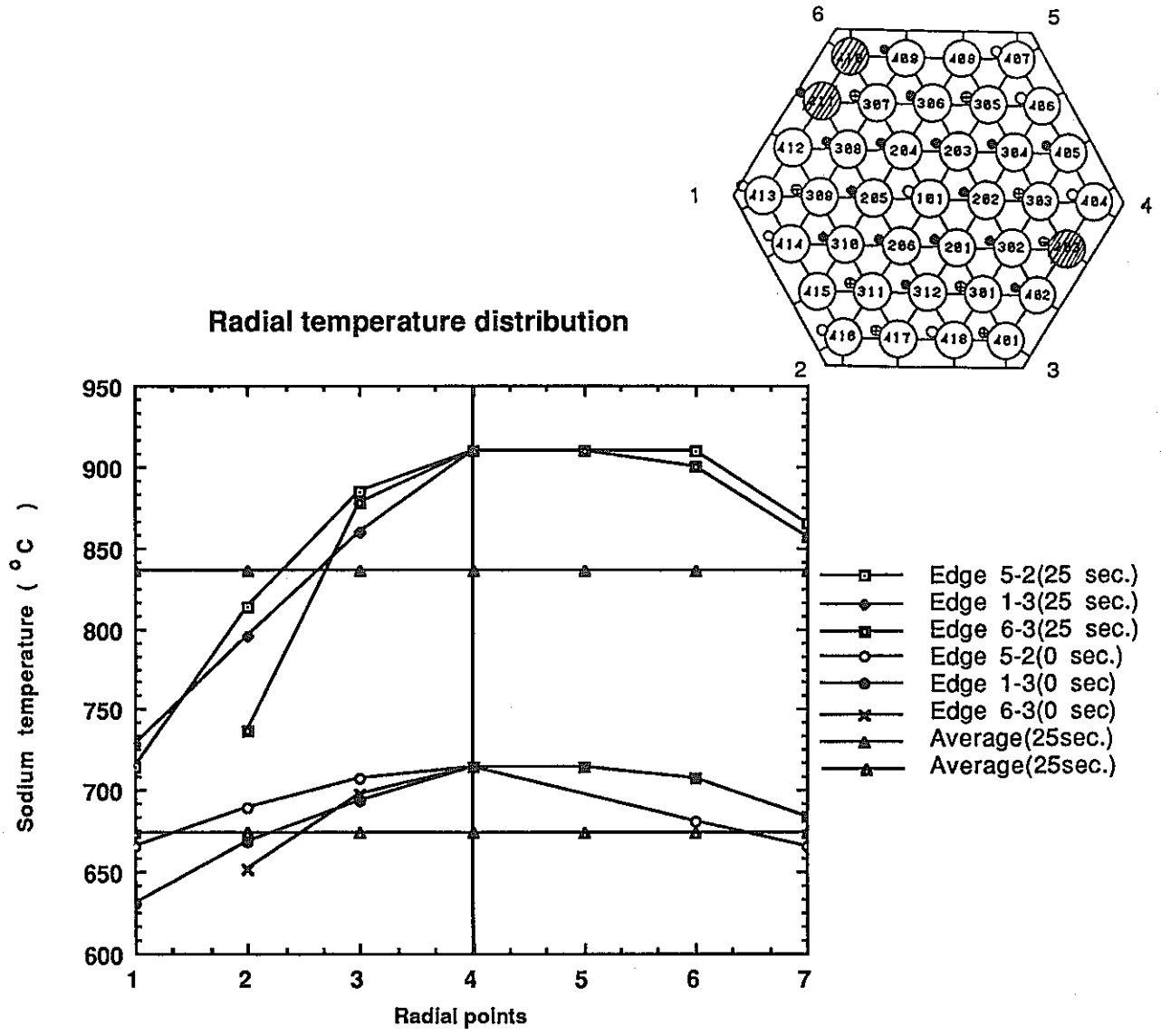

Figure 2.11 Radial temperature distribution before boiling.

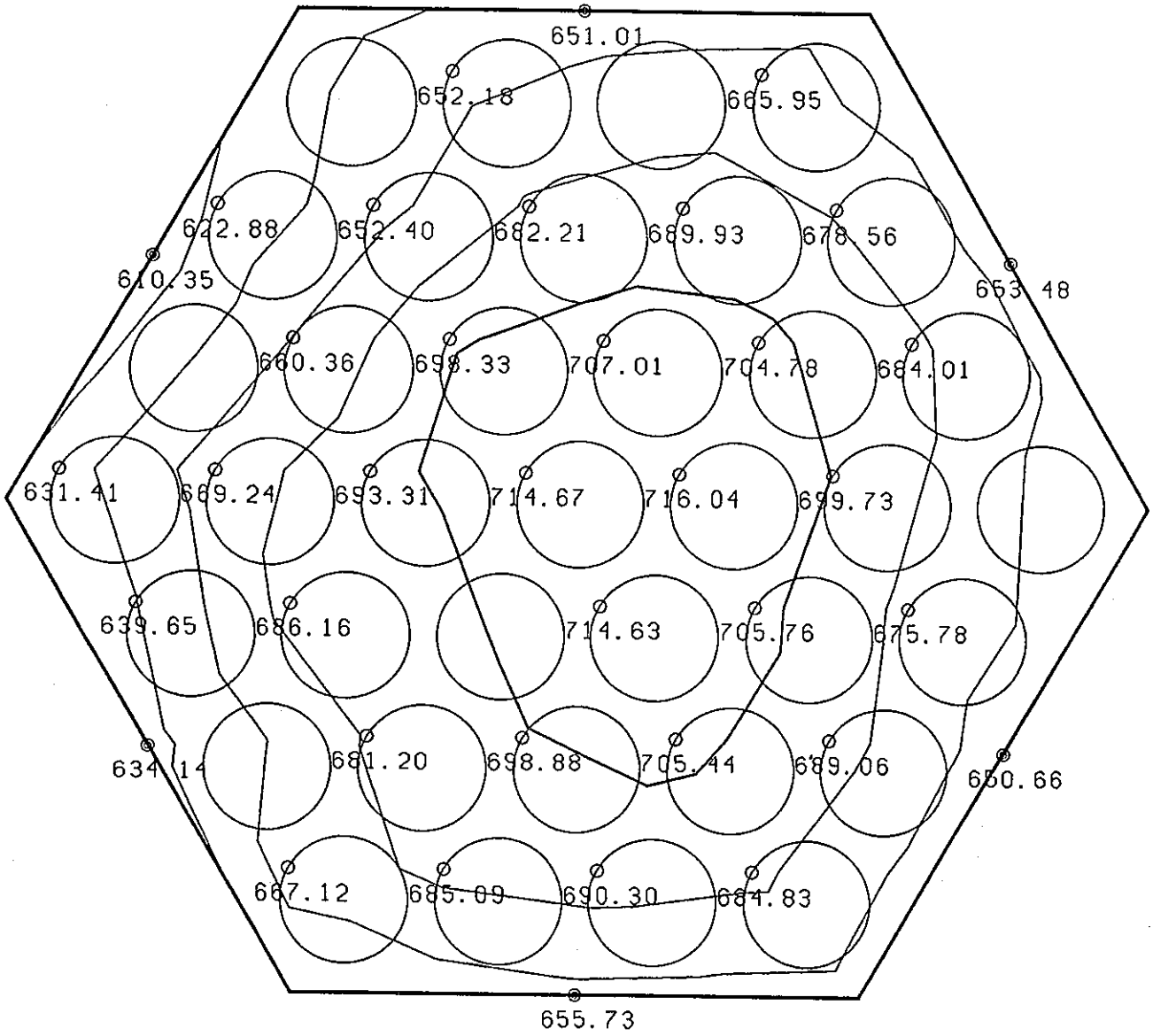

Temperature in deg. C

Figure 2.12 Sodium radial temperature mapping curve at the top of heated section from the initiation of transient. 0.0 sec.

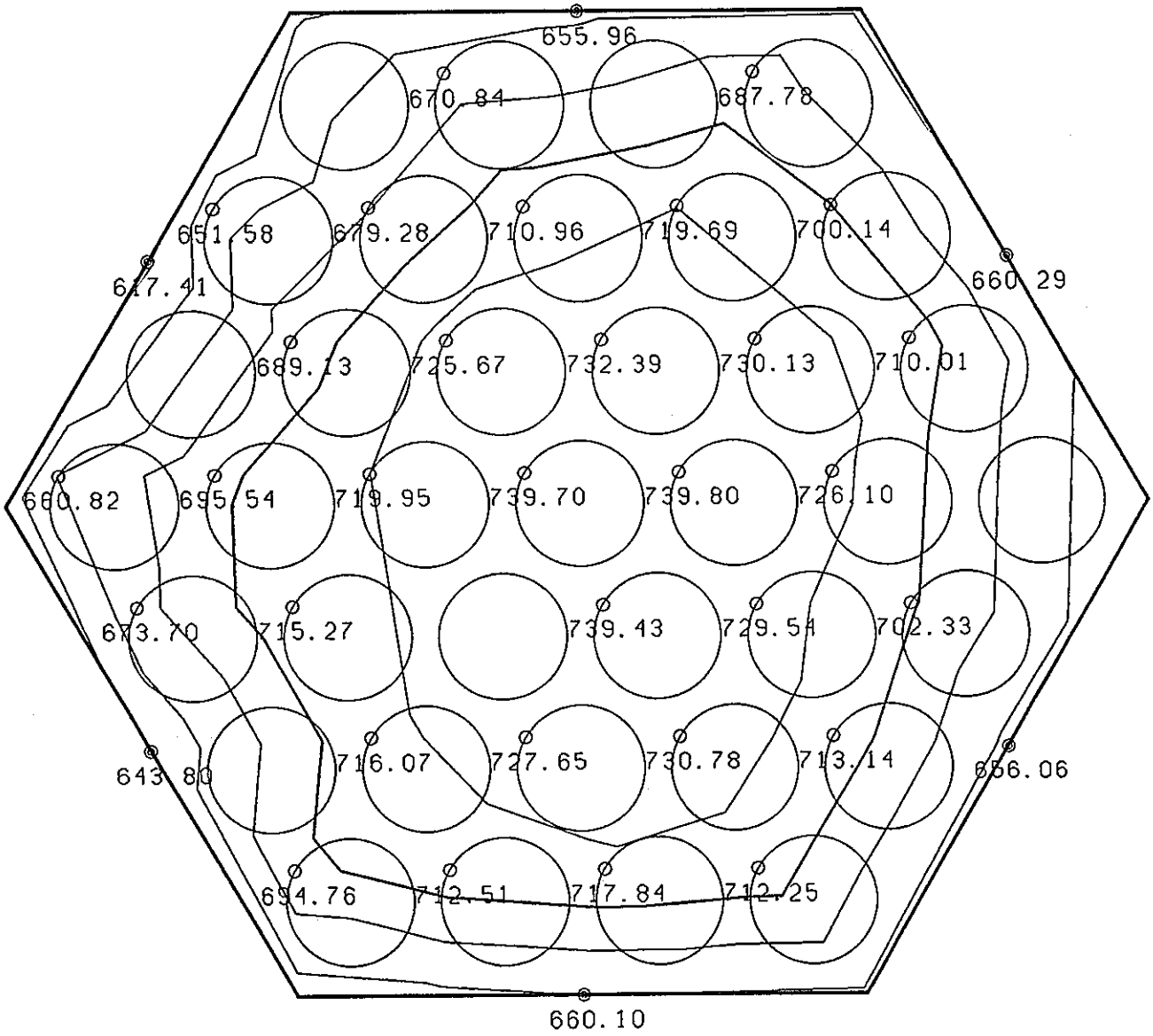

Temperature in deg. C

Figure 2.12 (continued) 5.0 sec.

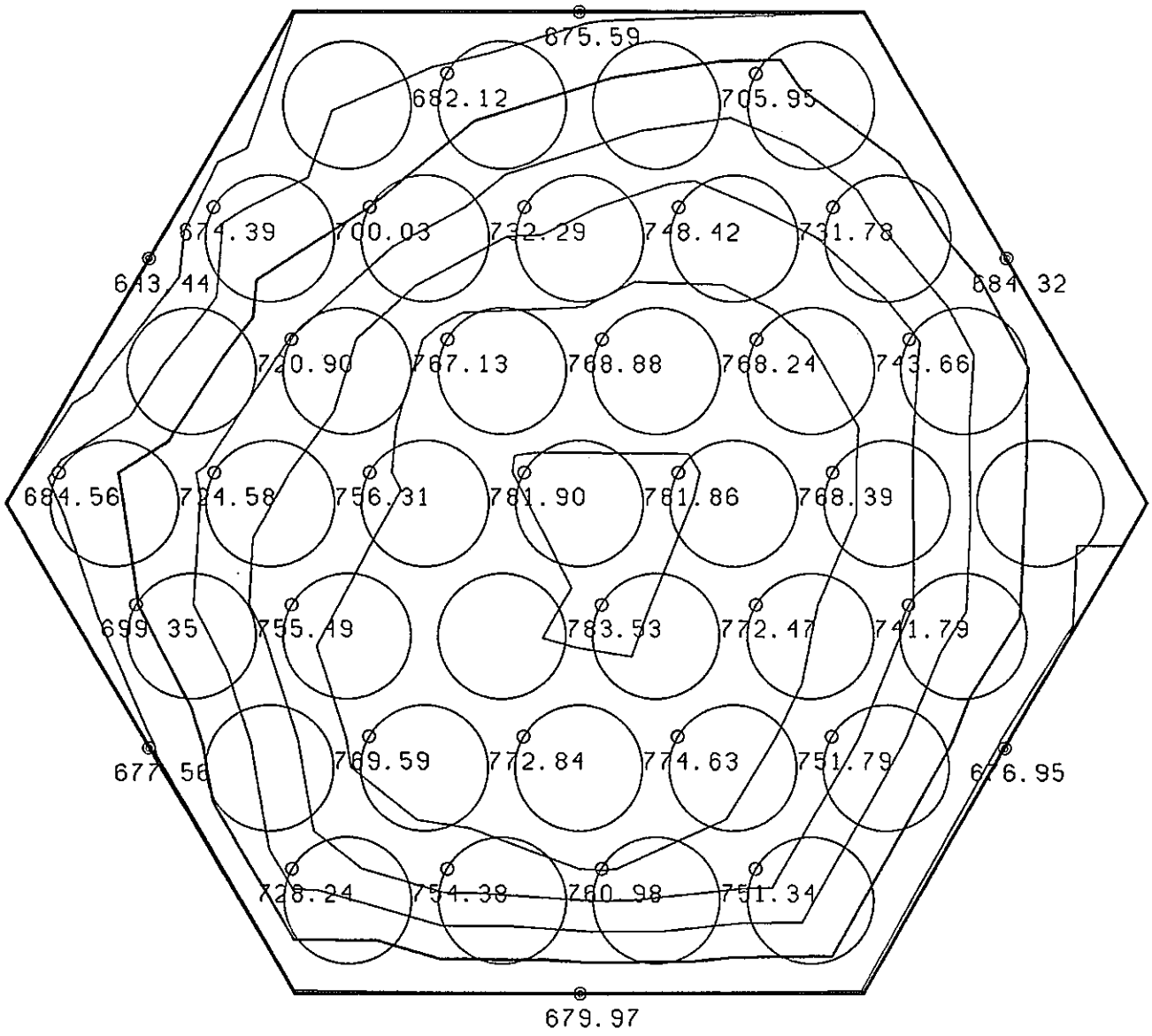

Temperature in deg. C

Figure 2.12 (continued) 10.0 sec.

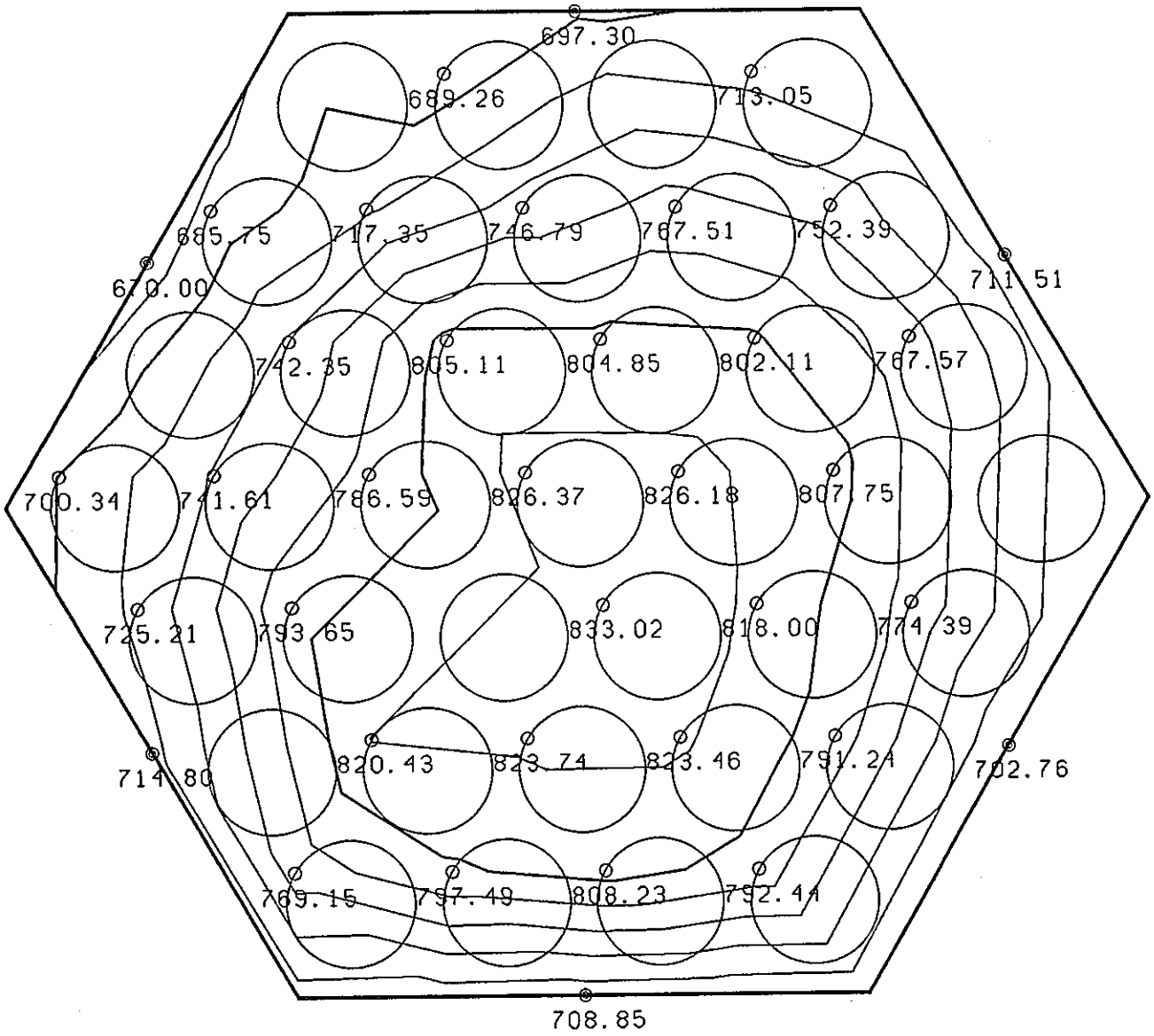

Temperature in deg. C

Figure 2.12 (continued) 15.0 sec.

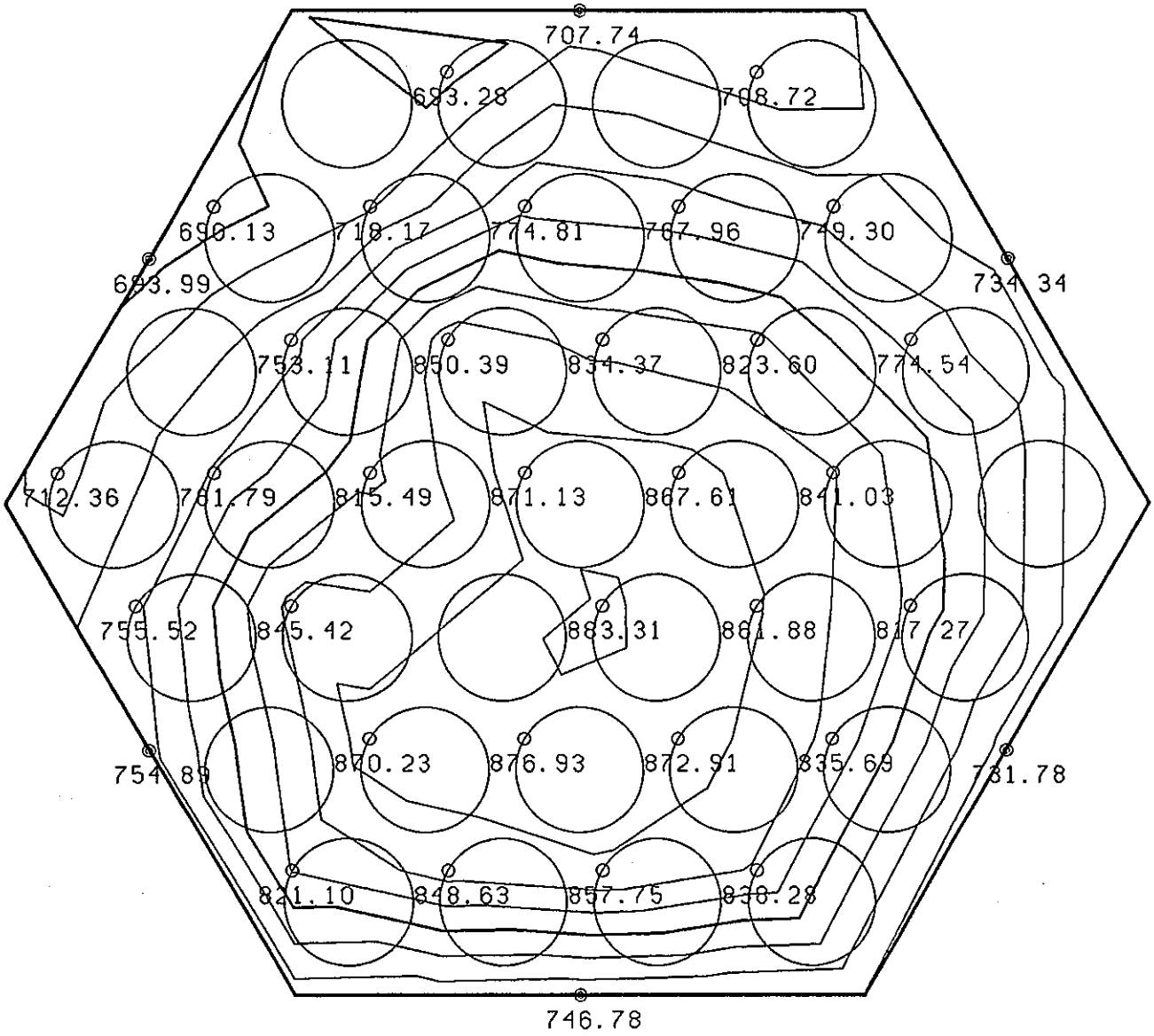

Temperature in deg. C

Figure 2.12 (continued) 20.0 sec.

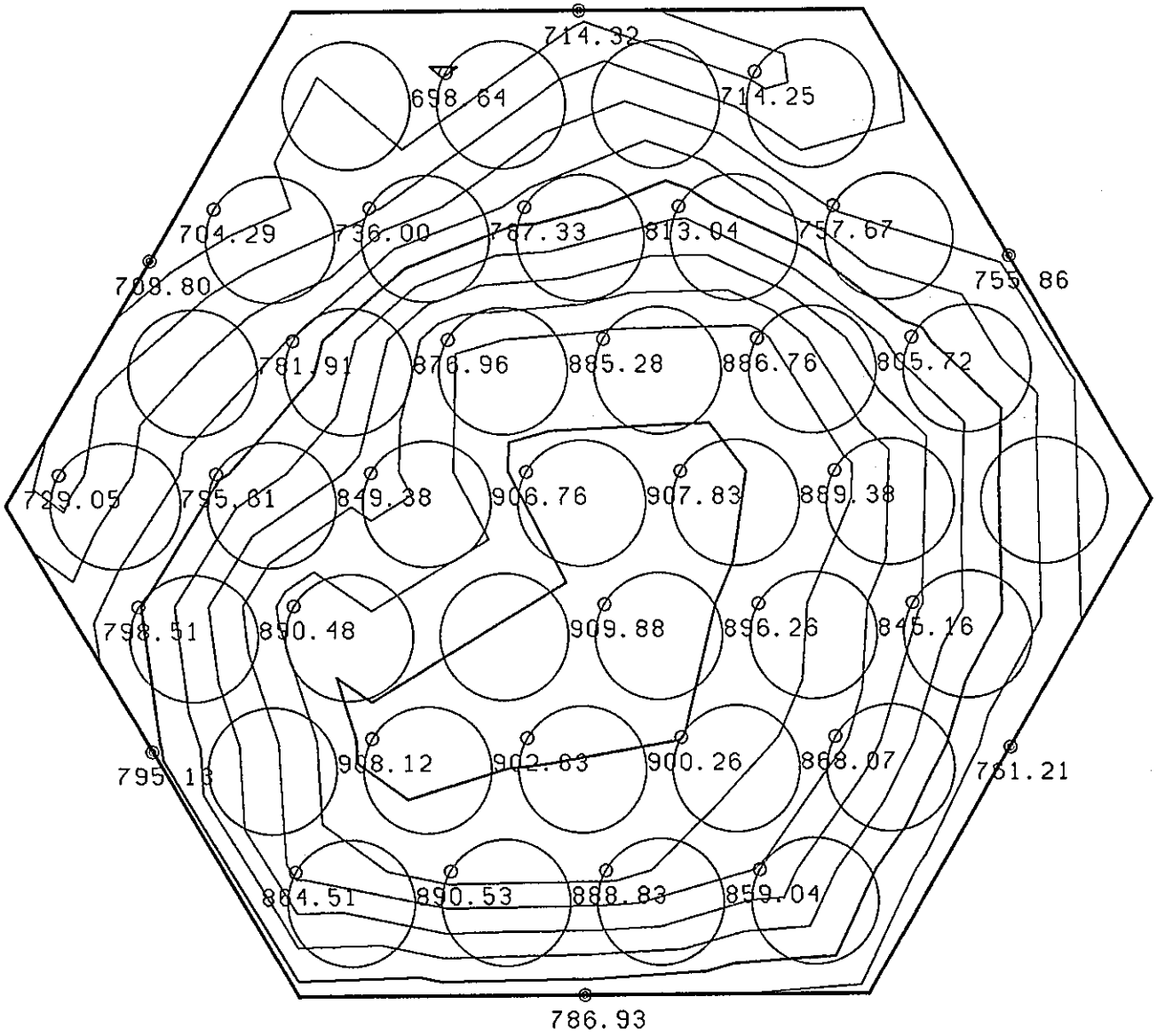

Temperature in deg. C

Figure 2.12 (continued) 25.0 sec.

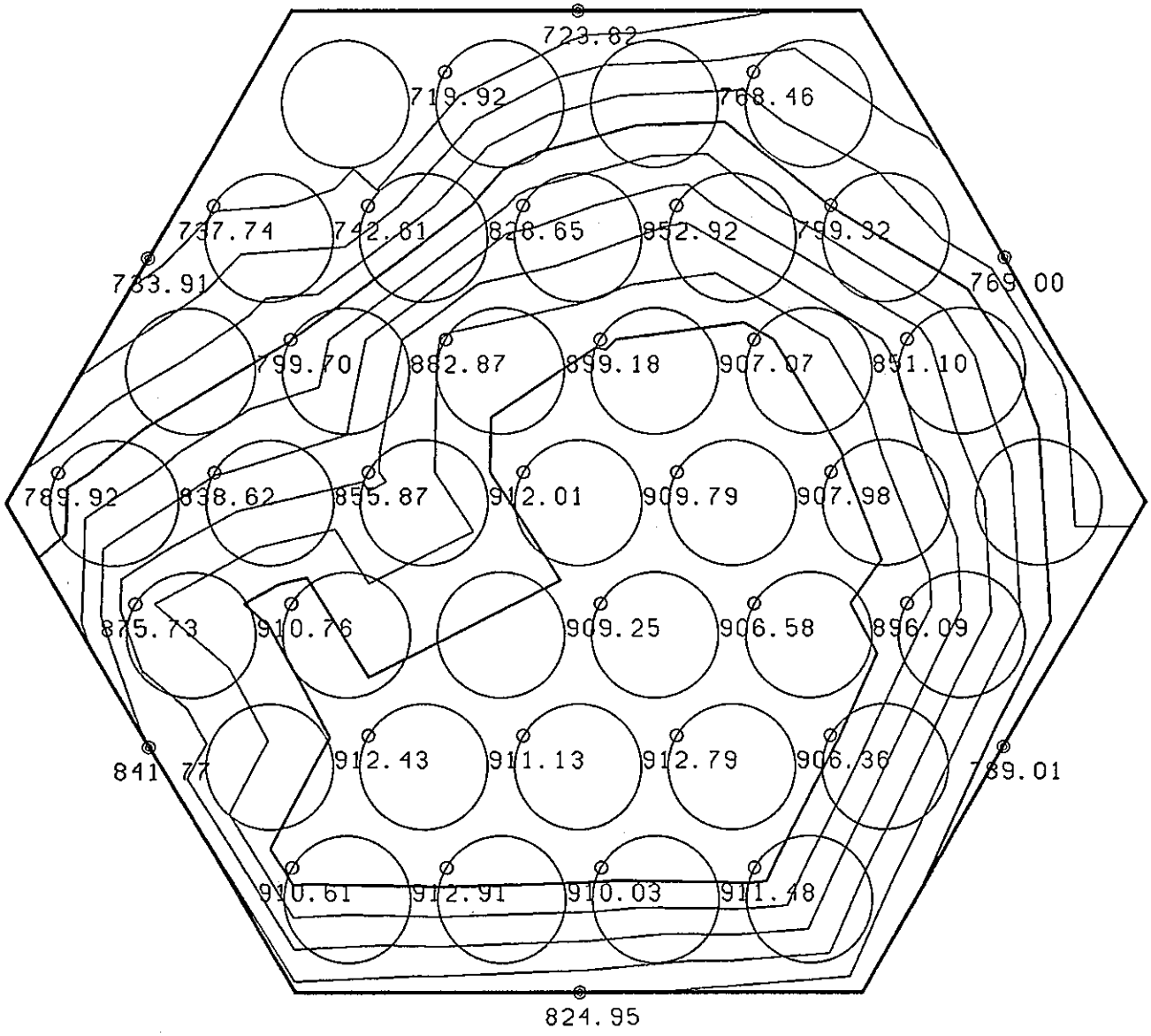

Temperature in deg. C

Figure 2.12 (continued) 30.0 sec.

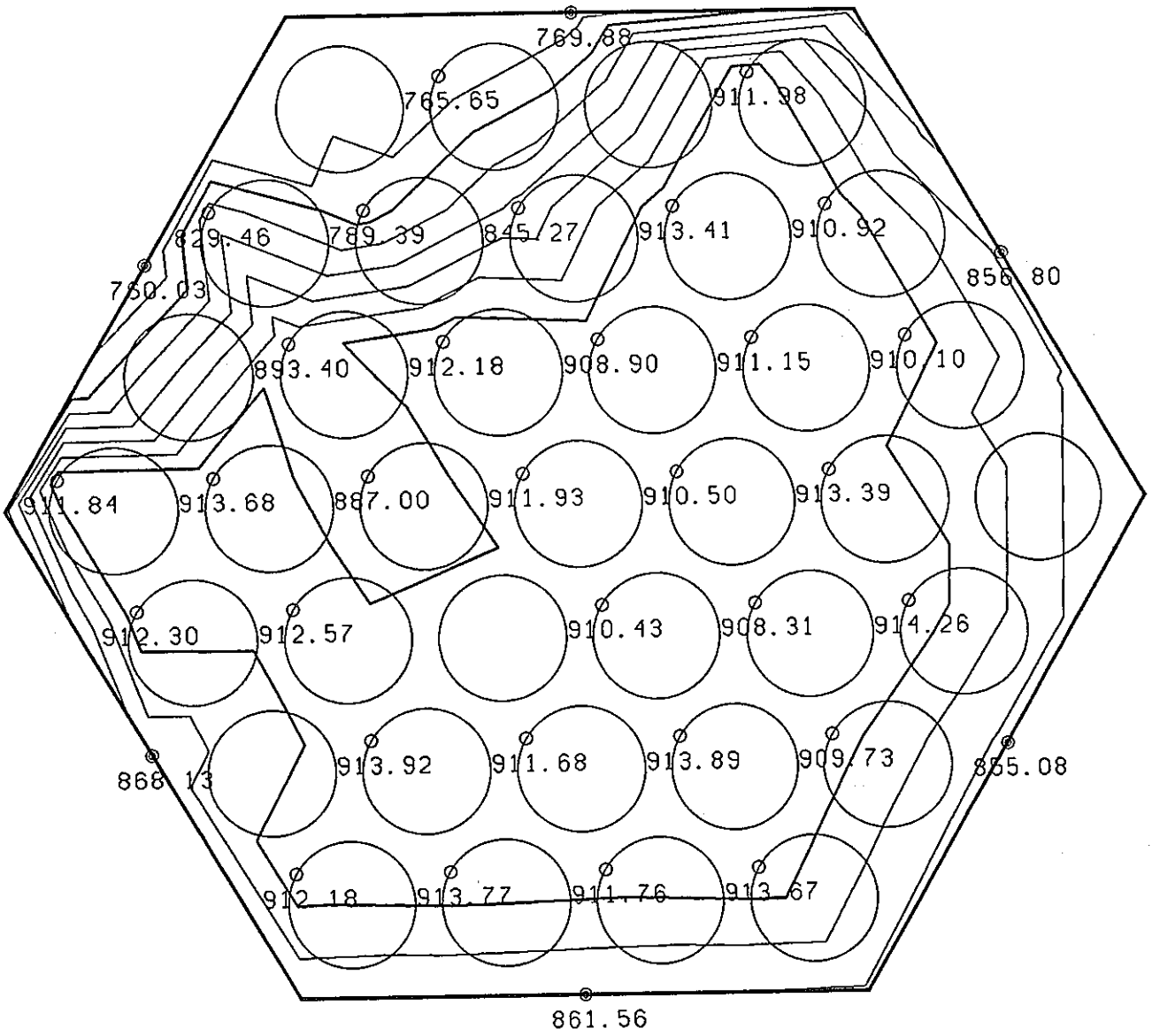

Temperature in deg. C

Figure 2.12 (continued) 35.0 sec.

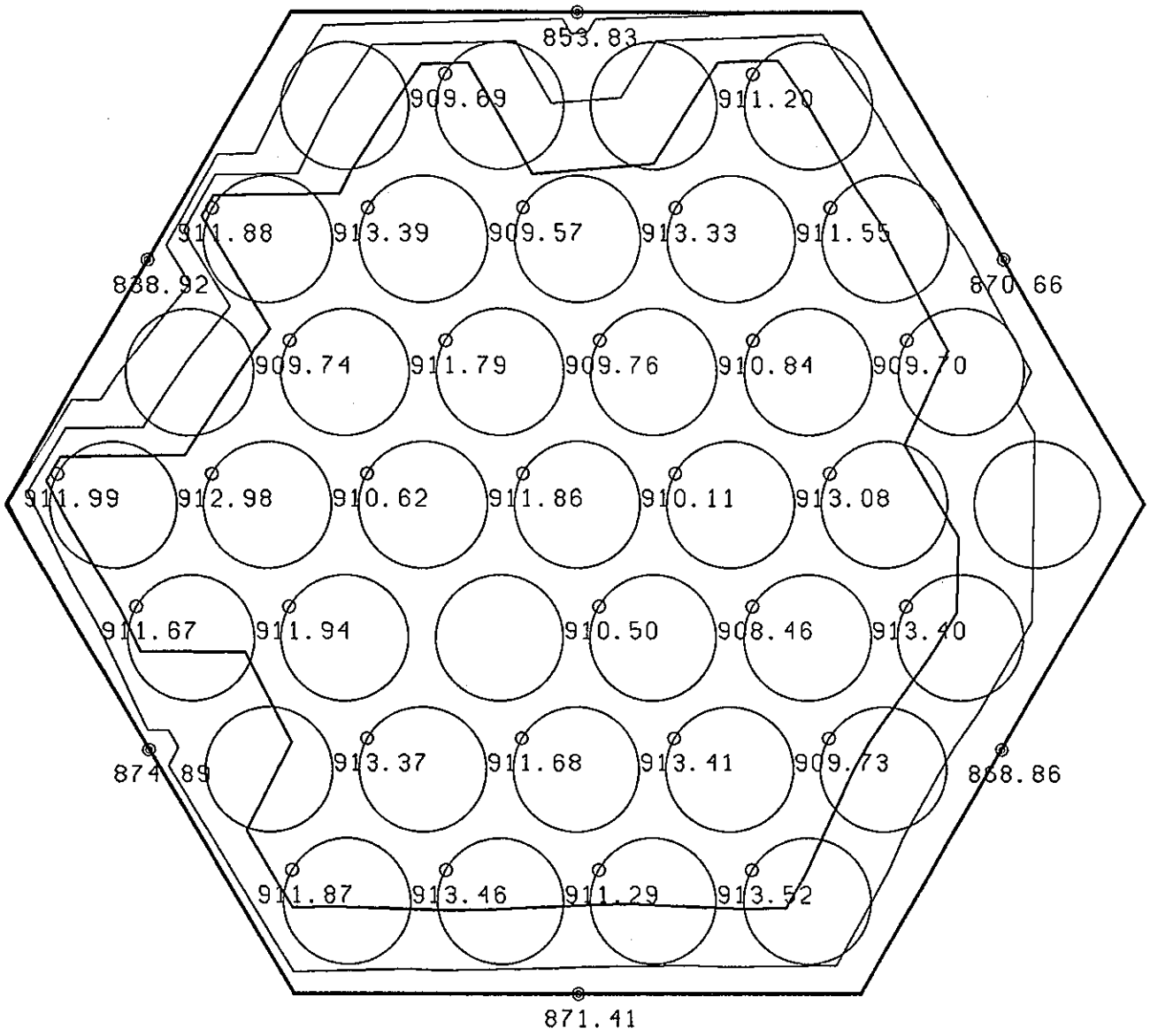

Temperature in deg. C

Figure 2.12 (continued) 40.0 sec.

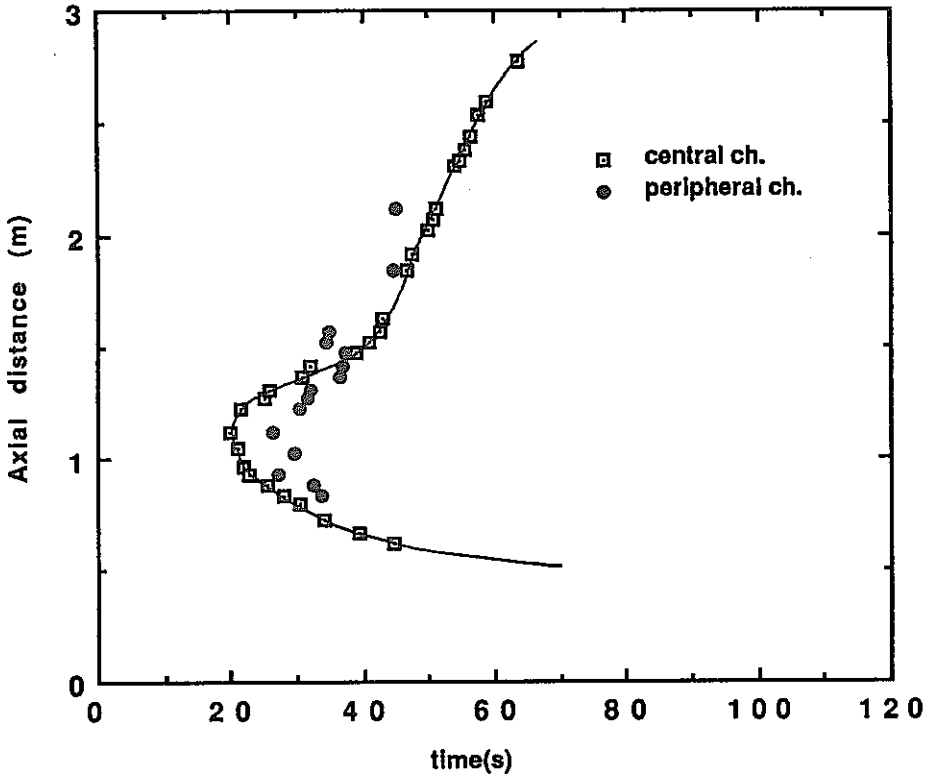

Figure 2.13 Axial void progression curve.

3.Analysis of PLANDTL LOF - 15057 experiment by SSC :

3.1. Introduction :

The simulation of a liquid metal cooled fast breeder reactor (LMFBR) plant for a variety of off normal and accidental condition is an important part of the overall safety evaluation. Super system code is a computer code which analyze the fast breeder reactor plant dynamic analysis under operational or accidental conditions . It was originally developed at Brookhaven National Laboratory. It has two version : 1) loop version SSC-L 2) pool version SSC-P. The loop version has been modified and improved at PNC and is being used for the safety analysis of LMFBR at OEC, PNC. SSC is also being used to analyze various experiments carried out in the PLANDTL facility to validate the analytical capability of the code.

In SSC, as a starting point of any transient calculation, a stable and unique steady-state or pretransient solution for the entire plant is obtained. In doing so, the time-independent form of continuity,energy and momentum conservation equations are reduced to a set of nonlinear algebraic equations. These equations are solved in two steps: first, the global parameters are obtained, then more detailed characterization is done by using the global conditions, obtained in the first step, as boundary conditions.

The energy and momentum conservation equations which describe the coolant flow in the tertiary loop are coupled since the constitutive laws depend explicitly on fluid pressure. These equations are represented in the form of a set of algebraic equations for each control volume. These equations are then solved iteratively for the steam generating system.

For sodium loop, the energy and momentum conservation equations may be decoupled when the effect of pressure on subcooled liquid

sodium properties is neglected. Therefore, the energy equations for both primary and intermediate heat transport system are solved in conjunction with the detailed solution of the steam generator. The head requirement for the sodium pump is then determined by computing the entire pressure drop in the loop. the actual pressure at any location in either the primary or secondary system is then related directly to the cover gas pressure

The numerical integration of the transient form of governing equation is done using a multiple time step scheme. In this method, different processes are integrated by using different time step sizes. This is achieved by dividing the entire system into a number of subsystems. Each of these subsystems uses different time step advancement. In order to keep logic required for integrating the different subsystem manageable, a total of four different timestep sizes are used. These are (1) hydraulic response of both the primary and intermediate heat transport system, (2) thermal response of both the primary and intermediate heat transport system, (3) fuel rod heat conduction and power generation computation and coolant dynamics in the reactor core, and (4) computation in the heat generation system.

Individual processes are solved by the numerical algorithm that is most suitable for the process under consideration. The overall interfacing of all processes is achieved by matching boundary conditions at the respective interfaces. The overall time step is controlled by requiring solutions to be numerically stable as well as by user specified accuracy criteria. A feature that is built in to the code allows the time step sizes to be automatically reduced or increased.

In SSC, the two-phase flow is analyzed by the homogeneous model which is also known as the mixture model. This model is the simplest representation for the mixture but is confined by three restriction of equal phasic pressures, temperatures and velocities.

3.2. Analysis of LOF -15057 by SSC.

PLANDTL loss of flow (LOF) experiment 15057 was simulated by SSC

to analyze the boiling behavior of sodium inside the test section. The input data was prepared for this experimental condition. Fuel pin was divided into 17 axial computational cell with cell no. 9 being the top of the heated section. We tried to simulate the transient phenomena for 120 second but the computation stopped at about 56 second of the transient time due to dry out of the heater pin surface. Figure: 3.1 shows the experimental and predicted flowrate vs. transient time curve. Figure:3.2 shows the SSC calculated temperature curve at the top of the heated section. Figure 3.3 shows the calculated quality, void fraction & two-phase friction multiplier curve. Later we will compare these curves with that we have found after the modification of the code.

From the temperature curve we find that boiling started at the top of the heated section about 28 second after the initiation of transient which is a little later than the experiment. From the void fraction curve, we find that due to large variation of density between the liquid phase and gaseous phase, as soon as boiling starts, void fraction reached to a very high value.

As we have discussed earlier that SSC employs homogeneous model for analyzing the two-phase flow in which it is assumed that both the phases are well mixed and travelling with the same velocity. But this assumption is not appropriate specially for the low pressure liquid metal cooled system where a very small value of quality corresponds to a very high value of void fraction due to the large difference in density between the two-phases and results in very high velocity of the vapor compared to the liquid velocity. So, the concept of well mixing of the two-phases is not the real situation in side the test channel. As a result SSC could not simulate the thermohydraulic behavior within the test section for this particular low pressure, low flow sodium boiling experiment.

3.3. Discussion of recent void and two-phase friction model and comparison with the SSC model :

In order to check the effect of void fraction (vf) and two-phase friction multiplier model (tpfm) we decided to use recent models in SSC. Before selecting the model to be applied, we will discuss briefly about the various void and two-phase friction multiplier

models available.

As we know, reliable application of two-phase flow models depends on the accurate prediction of two-phase pressure drop. Analysis of two-phase flow pressure drop is vastly more complicated than that for single phase flow. This is due to the multidimensional variation in mass and velocity distribution, further hampered by nonuniformity in heat transfer in convection two-phase flow.

Generally, The two-phase pressure drop in a vertical tube of length dz is composed, when written in differentials, of the sum of three terms

$$\left(\frac{dp}{dz}\right)_{2ph} = \left(\frac{dp}{dz}\right)_{f,2ph} + \left(\frac{dp}{dz}\right)_{a} + \left(\frac{dp}{dz}\right)_{g}$$

In this series, the terms take account of the two-phase friction pressure loss, the acceleration pressure drop and the hydrostatic pressure drop. The last two terms are defined as

$$\left(\frac{dp}{dz}\right)_{a} = -m_d^2 \frac{\partial}{\partial z}\left(\frac{(1-x)^2}{\rho_l(1-\alpha)} + \frac{x2}{\rho_v \alpha}\right)$$

$$\left(\frac{dp}{dz}\right)_{g} = -\,g\,\{\alpha\rho_v + (1-\alpha)\,\rho_l\}$$

where m_d is the mass flow density, x the mass flow vapor quality, ρ_l and ρ_v are the density of the fluid and the vapor respectively, α is the void fraction and g is the acceleration due to gravity. So the calculation of a total pressure drop depends on the accurate knowledge of the friction pressure loss and of the void fraction.

Now, two-phase pressure gradients are often expressed in term of a two-phase multiplier. Thus

Two-phase pressure gradient = single phase pressure gradient X two phase multiplier

A number of models are available to predict the friction multiplier. In SSC, homogeneous model two-phase friction multiplier(tpfm) and void fraction (vf) model are used. P. B. Whalley in his book Boiling, condensation and gas liquid flow gave the following view on the homogeneous model

Homogeneous model gives good result of frictional pressure gradient if $\rho_l/\rho_v < 10$ or if $m_d > 2000$ kg/ m^2 s.

Homogeneous void fraction is a good estimate of the actual void fraction if $\rho_l/\rho_v < 10$ or if $m_d > 2000$ Kg/ m^2 s

From the above discussion we find that homogeneous model can give reasonable prediction at high pressure and mass flux. In case of PLANDTL LOF - 15057 experiment the mass flux is very low which is about 7kg / m^2 s and ρ_l/ρ_g is about 2150. So it is evident that the prediction of SSC of frictional pressure gradient and void fraction by the two-phase model is not accurate enough to simulate the actual flow condition of the experiment.

Among the other correlations available, the most widely used correlation for the calculation of two-phase multiplier is that of Lockhart and Martinelli. However, there exists various shortcomings of this correlation and found to be inadequate in representing a wide range of two-phase pressure gradient data and large mean and standard deviation are observed when the models are compared with large bank of experimental data. Typical standard deviation may range upto 100 percent.

Over the years, continuous efforts have been made to derive better correlation for frictional pressure gradient. As more data become available, the deficiencies of other correlation became apparent and further correlation were developed. This process is a continuing one and it reflects the fact that for a situation as complex as two-phase flow, it is very difficult to formulate relationship that have general physical basis. The main difficulty is that the empirical correlation are based on the assumption that the frictional pressure gradient is function only of channel cross sectional geometry, mass flux and physical properties. However in two-phase flow, the effect of flow development is very considerable any wide ranging data bank on two-phase flow contains data with a variety of inlet configuration and channel length, which will give a range of pressure gradients for the same nominal conditions. The length required to reach equilibrium in two-phase flow corresponds typically to several hundred diameters and thus most experiments never reached

equilibrium conditions. Furthermore in practical situations equilibrium conditions themselves are not relevant, particularly when there is a phase conversion along the channel.

Recently, Friedel gave a complicated empirical equation for the two-phase pressure gradient which is applicable to any fluid , except when $\mu_l/\mu_g > 1000$. It has been described as the best generally available and generally applicable correlation. It is given in Appendix A. We decided to use this correlation in the SSC two-phase flow model.

For void fraction determination, it has been found by study that Lockhart- Martinelli type correlation do not fit void fraction data well. This correlation also.does not take care of the effect of mass flux So we decided to use another correlation proposed by Premoli et. al which covers a reasonably wide range of data and takes account of the mass flux effects. This correlation is based on slip ratio. It is given in Appendix B.

3.4.Analysis of LOF - 15057 by SSC after incorporating the recent void and pressure drop model :

The CISE void fraction determination correlation and the Friedel two-phase friction multiplier correlation were incorporated into the original SSC and we tried to simulate the PLANDTL LOF- 15057 experiment but calculation stopped at 58th. second of the transient time due to dryout of the channel. So, after the use of the two best available correlation for void fraction and two-phase friction multiplier, no significant improvement of the result was achieved. Figure 3.4 shows the calculated quality, void fraction & two-phase friction multiplier curve after the modification. From the curve, we find that Friedel correlation gives a higher value of two-phase friction multiplier compared to the previous model of SSC. It is evident from the quality vs void fraction curve (Figure 5.1) that from the initiation of boiling upto a certain value of quality, Friedel tpfm is larger than the SSC calculation. As a result, the two-phase pressure drop also become higher at the beginning, which ultimately leads to high quality boiling as seen from the quality curve. But since CISE correlation for void fraction determination gives a lower

value of void fraction for different quality level (Figure :5.2), it results in a slight delay in reaching the dry out state. Like the previous calculation by SSC without any modification, we find that boiling starts at about 28th second of the transient at the top of the heated section and this result is in good agreement with the experimental result. After the initiation of boiling, for the low quality boiling region, the homogeneous model of SSC predicts the boiling behavior accurately as seen from the calculated mass flow curve and as the quality increases homogeneous model overestimates the two-phase pressure drop which results in dryout of the channel.

So we can conclude that, the homogeneous two-phase model of SSC is good in simulating the low pressure, low flow, low quality boiling behavior of sodium but for high quality boiling, it can not analyze the thermohydraulic behavior properly.

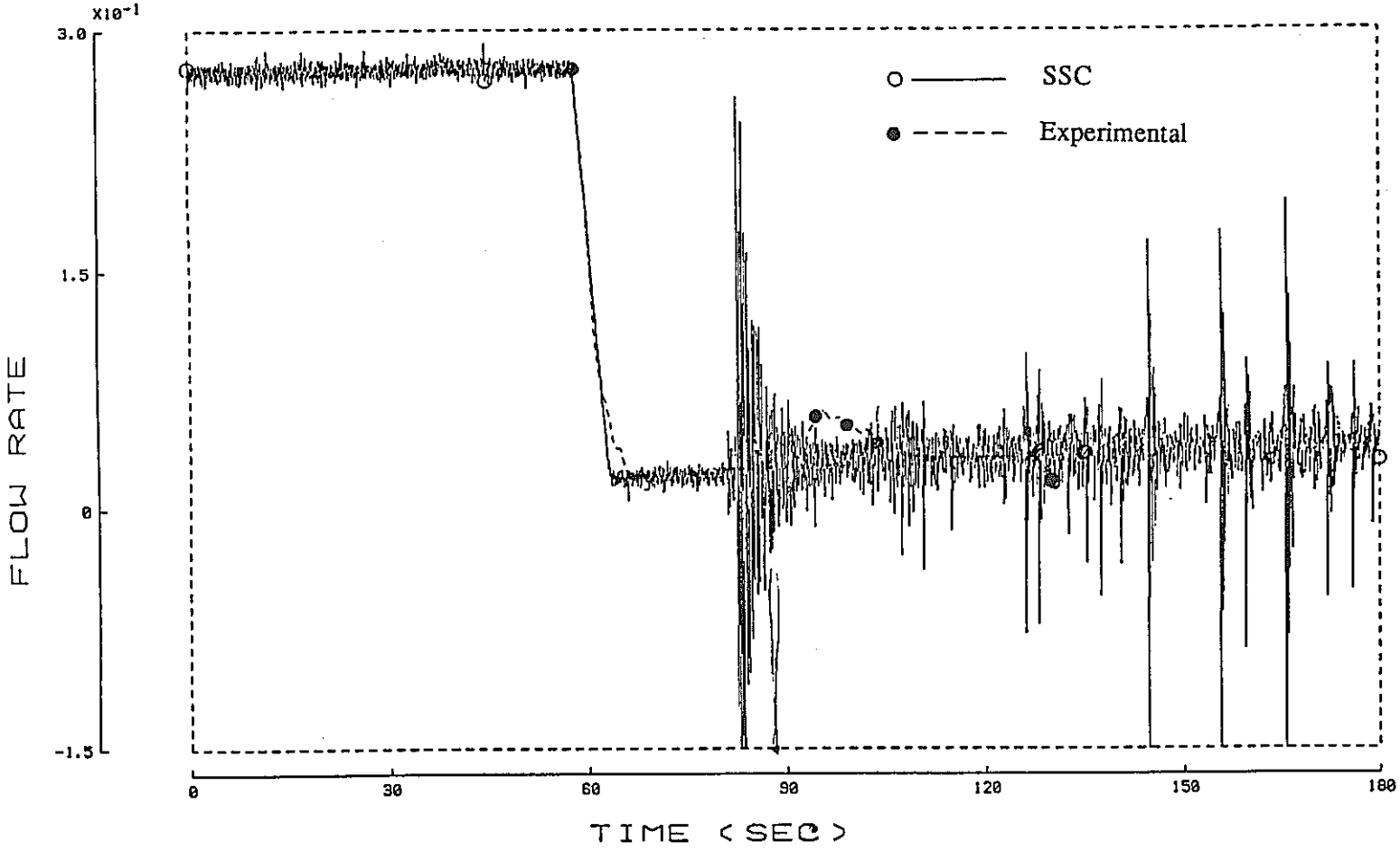

Figure 3.1 Experimental & predicted flowrate vs.time curve.

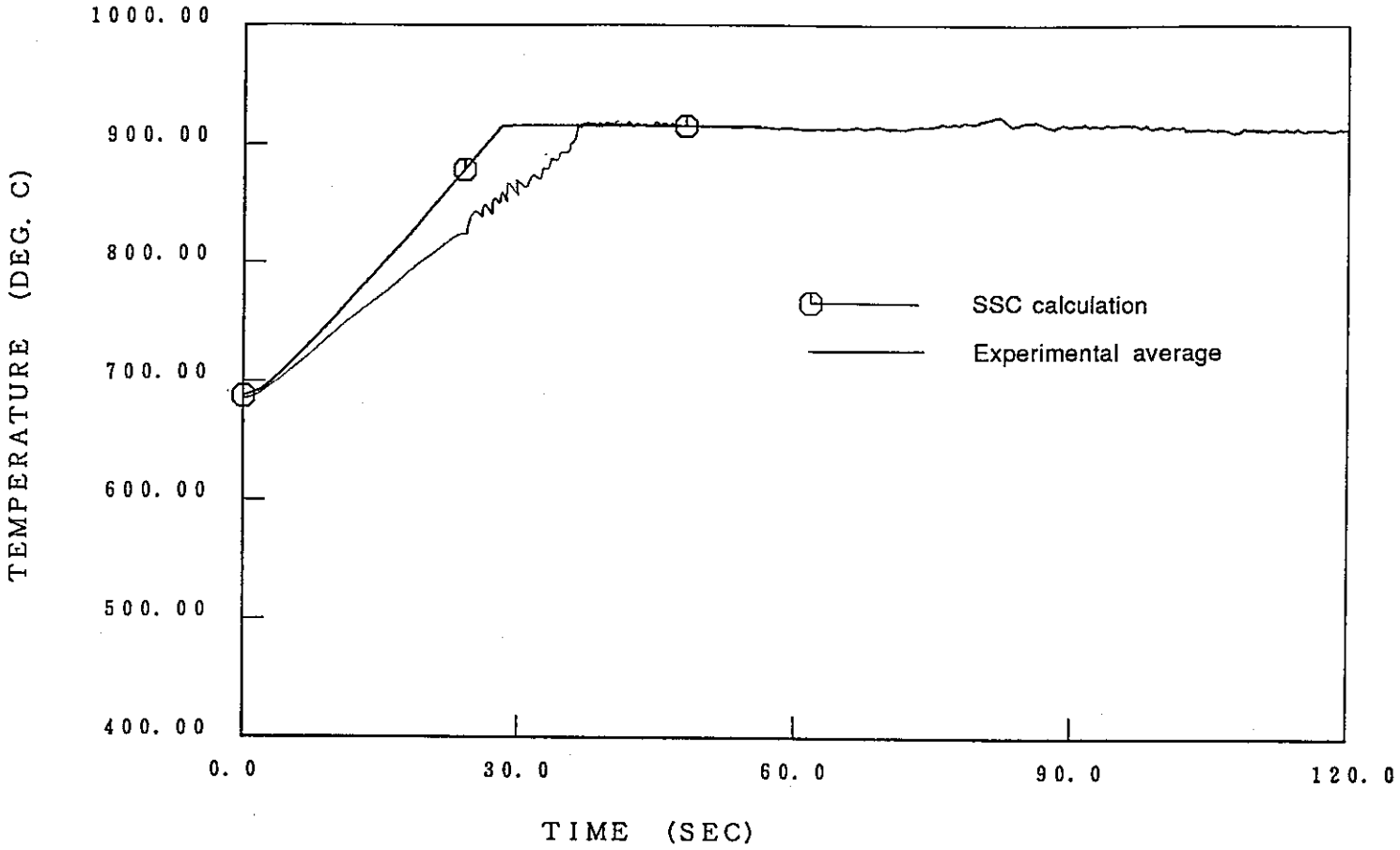

Figure 3.2 Calculated and experimental average temperature vs.time.
(Top of the heated Section)

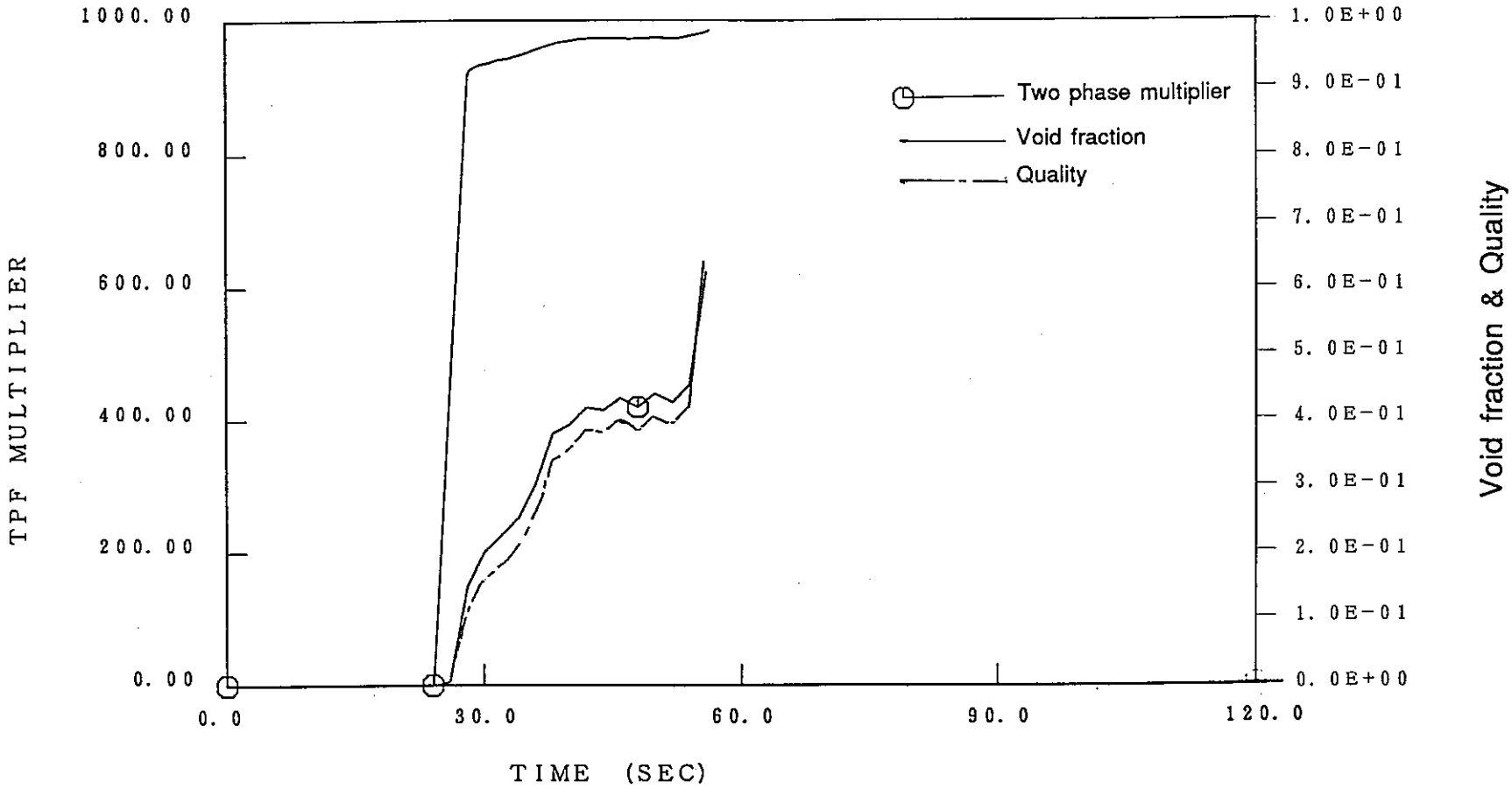

Figure 3.3 Calculated quality, void fraction & two phase friction multiplier vs. time curve.

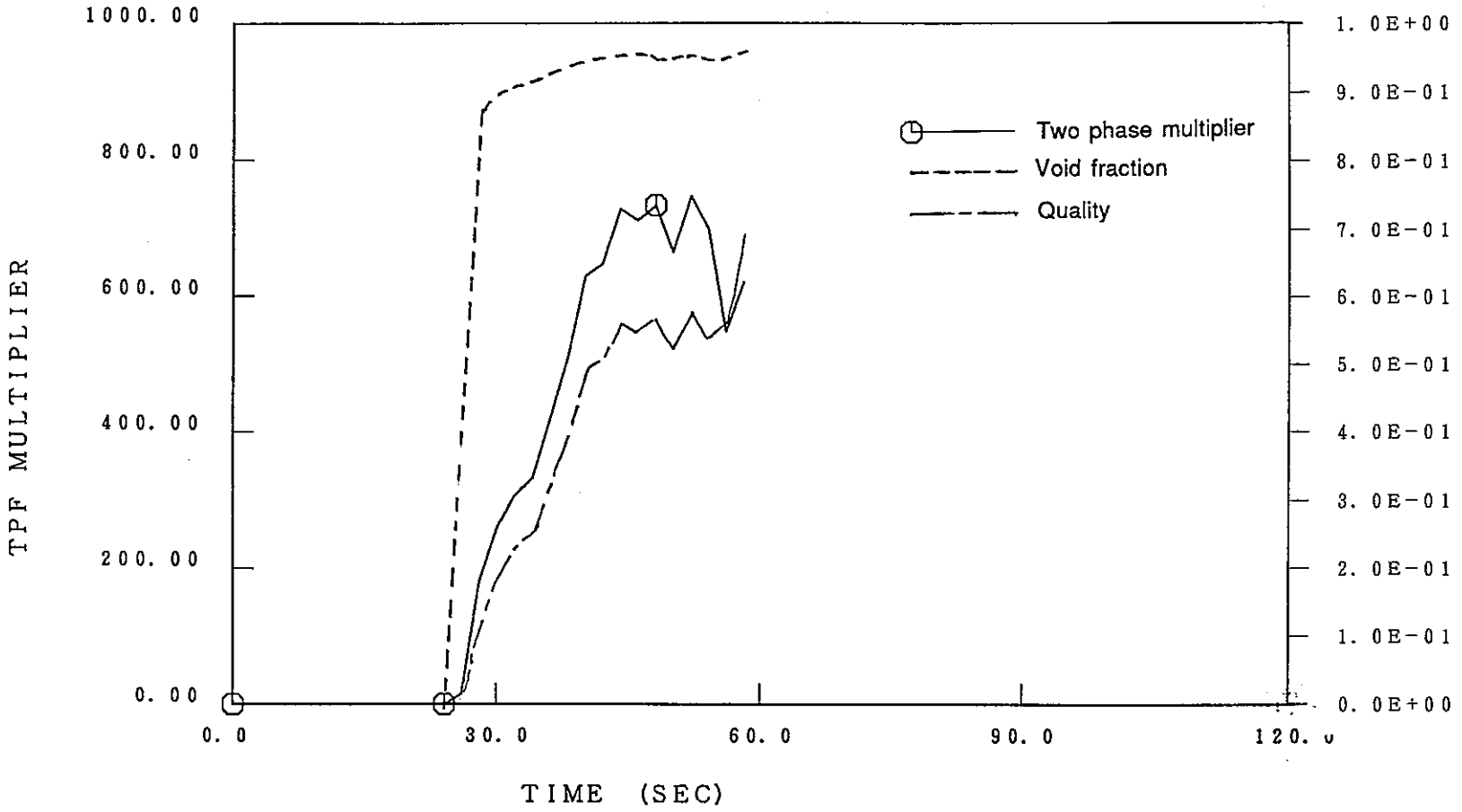

Figure 3.4 Calculated quality, void fraction & two phase friction multiplier vs. time curve (after modification).

4. Analysis of PLANDTL LOF - 15057 experiment by SABENA 1-D :

4.1. Introduction :

In case of liquid metal cooled fast breeder reactor (LMFBR), under low pressure operating conditions, large liquid to vapor density ratio induces an abrupt mixture density change followed by highly nonequillibrium phenomena. The existence of highly subcooled sodium surrounding the boiling region within the fuel bundle causes vapor condensation which is one of the key phenomena that directs the local and global coolant dynamics. In general the boiling from its initiation upto dryout on pin surface exhibits a spatially incoherent behavior. In view of the above consideration of the liquid boiling characteristics, Two-fluid two-phase model approach of analysis is the most appropriate.

As a contribution to the LMFBR safety analysis associated with the loss of flow (LOF), loss of piping integrity (LOPI) and two-phase flow produced by an extreme power and flow mismatch in the fuel subassemblies of the core , computer code SABENA (SubAssembly Boiling Evolution Numerical Analysis) has been developed at the reactor engineering section of the OEC, PNC to simulate the thermohydraulic behavior of the coolant in fuel pin bundles under various accidental and transient condition using the Two-fluid two-phase separated flow model.

In SABENA code, the Two-fluid model is formulated in terms of two set of conservation equation governing the balance of mass, momentum and energy of each phase. Since the macroscopic field of one phase is not independent of those of other phase, the interaction term that couple the transport of mass, momentum and energy of each phase across the interface appear in the field equation. In Two-fluid model representation, the transport process of each phase are expressed by their own balance equations. Therefore it can

predict more detailed changes and phase interaction than a mixture model like SSC.

SABENA code has been developed in two versions. One is the one dimensional version (SABENA-1D) and the other being its subchannel version SABENA 3-D which includes two dimensional analytical capability.

4.2.1. Two-fluid model of SABENA :

In SABENA code, the thermofluid dynamics of sodium boiling and two-phase flow is described by the six basic conservation equations for mass, energy and momentum of each phase of fluid. In the following, a set of simplified local volume averaged Two-fluid six equation system is given.

conservation of mass :

$$\frac{\partial}{\partial t}(\rho_j\alpha_j) + \nabla\cdot(\rho_j\alpha_j u_j) = \Gamma_j$$

conservation of energy :

$$\frac{\partial}{\partial t}(\rho_j\alpha_j e_j)+\nabla\cdot(\rho_j\alpha_j e_j u_j)=-p\left\{\frac{\partial\alpha_j}{\partial t} + \nabla\cdot(\alpha_j u_j)\right\} + Q_{wj} + Q_{ij} + Q_{kj}$$

Conservation of momentum :

$$\frac{\partial}{\partial t}(\rho_j\alpha_j u_j) + \nabla\cdot(\rho_j\alpha_j u_j u_j) = -\alpha_j\nabla p - F_{wj} - F_{Ij} - F_{\Gamma j} - \rho_j\alpha_j g$$

Interface jump condition :

$$\sum_j \Gamma_j = 0$$

$$\sum_j F_{Ij} = 0$$

$$\sum_j Q_{Ij} = 0$$

where the subscript j refers to g (vapor phase) or f (liquid phase), ρ_j, α_j and u_j are the density, the volume fraction and velocity of the j-th phase respectively. Γ_j is the interface mass transfer, Q_{wj}, Q_{Ij} and Q_{kj} are the energy exchange between wall and j-th phase, the energy exchange between interface and j-th phase, and the energy transfer due to heat conduction in j-th phase of the fluid, respectively. F_{wj} and F_{Ij} are the momentum exchange of the j-th phase of the fluid with the wall and the interface. $F_{\Gamma j}$ is the momentum gain or loss due to the mass exchange of the j-th phase and g is the gravitational acceleration.

4.2.2. Boundary conditions and calculation features :

In the SABENA program, the fictitious cell are provided to accommodate the boundary conditions. For the top and bottom of the assembly two types of boundary conditions are considered namely the prescribed pressure and prescribed velocity. For the inflow boundary condition either velocity or pressure specification are provided along with void fraction, liquid and vapor temperatures. In case of outflow boundary condition pressure specification is provided.

The SABENA code allows to calculate : i) fuel pin heat conduction and heat transfer to the fluids, ii) wrapper wall heat conduction and heat losses to the atmosphere, and iii) external loop characteristics including the effect of pump, heat exchanger, plenum, piping etc. These models are coupled implicitly to the fluid analysis part. The third feature is important because boiling behavior in a bundle section are influenced strongly by external loop characteristics.

4.3. Analysis of LOF-15057 by SABENA 1-D and comparison with the experimental findings :

In order to simulate the LOF -15057 sodium boiling experiment by SABENA 1-D, the test section has been modeled by dividing the

entire bundle length into 42 computational cell, using equivalent hydraulic and heated perimeter and using total cross sectional area taking into consideration the effect of wire wrapping. The simulation was carried out by inflow velocity (bottom) and outflow pressure (top) boundary condition in order to duplicate the experiments inlet mass flow rate condition. Figure : 4.1 shows the experimental and calculational inlet mass flow velocity vs. time curve.

From the transient time vs. coolant temperature curve for different axial node (figure : 4.2) , we find that boiling is predicted to start at the top of the heated section of the test channel at about 35 second of the transient time. However as we have already discussed , from the thermocouple reading of the central region, boiling started at about 25 second. This difference in predicting the on set of boiling compared to the experimental condition is due to the following fact.

In one dimensional case, both the central and edge channel are represented by a single average temperature which is less than the maximum fluid temperature encountered in the central channel of the heated pin bundle i.e. radial temperature distribution in case of one dimensional approximation can not be encountered. From the radial temperature distribution curve for the top of the heated section just before the onset of boiling (figure:2.11), we find that although temperature of the central region almost reached the saturation level but temperature near the wall of the hexagonal wrapper tube was still much lower and the average temperature of the coolant was 836 deg. C. So it took some time for the entire channel to reach at the saturation temperature level and we find that at about 35 second of the transient time, saturation region reached near the wall of the the entire axial cross section at the top of the heated section and this is the time for the onset of boiling as predicted by the SABENA 1-D code.

Another reason for the early beginning of boiling inside the test channel compared to the experimental result is due to the effect of the presence of three unheated heater pin inside the test channel. As mentioned earlier, the test section power was kept at a constant 100KW level throughout the transient experiment period. This power output was the contribution from 34 heater pin. So the heat flux was much higher than it should be if all the heater pins were

operational. As a result, temperature of the central region reached the saturation level comparatively faster than normal. The effect of the three unheated pins were not taken into account in SABENA-1D calculation.

Figure : 4.3 shows the transient time vs experimental (average) and calculated sodium temperature curve for the top of the heated section and we find that these two curves agrees with each other. Figure : 4.4 shows the transient time vs. temperature of differnt radial position of the top of the heated section measured by the thermocouple and the average calculated temperature of that section by SABENA 1-D. This curve shows that peripheral radial position reached at the saturation temperature level much later than the central channel.

Figure : 4.5 shows the inlet pressure vs. transient time curve for experimental and calculational condition and we find that they almost agree with each other.

Figure : 4.6 shows the calculated axial void progression contour line vs. time . Actually this curve, based on the calculation of SABENA 1-D, represents the expansion of voided region when the boiling front reached edge channel of the test section. Since we have no such curve for the experimental situation so, it is not possible to compare this curve with the experimental condition but if we compare this curve with the experimental saturated temperature region axial expansion curve for the peripheral region which is a little bit far from the edge of the channel(figure 2.13), we could infer that this curve predicted the expansion quite accurately.

From the above discussion we can conclude that SABENA 1-D's calculation is in good agreement with that of PLANDTL LOF -15057 experiment if we consider the average temperature of the coolant calculated by the code with that of the experiment. The cross-sectional average temperature calculated by SABENA at the top of the heated section reached the saturation level almost at the same time if we compare it with the cross-sectional average temperature of the experiment at that instant. Regarding the axial expansion of

the voided region, SABENA 1-D predicts the expansion towards the upstream side quite accurately. The simulation continued for the prescribed time period with no dry out of the channel as was observed in the experiment. The onset of boiling, observed in the experiment, has not been predicted since radial temperature distribution can not be taken care of by one dimensional approximation. So SABENA 1-D simulates the thermohydraulic behavior within the test channel with sufficient accuracy considering the inherent shortcoming of the one dimensional model.

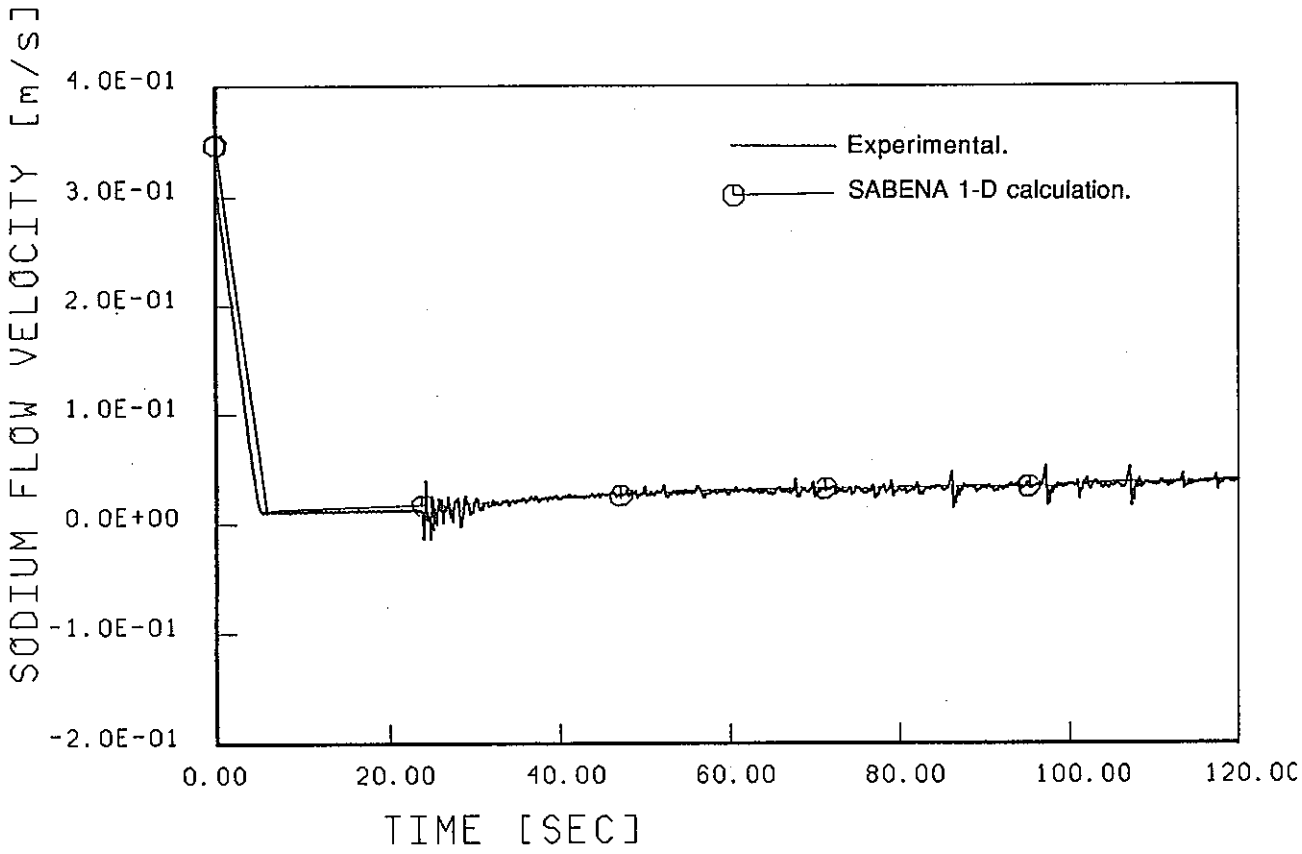

Figure 4.1 Experimental & calculated mass flow velocity vs. time curve.

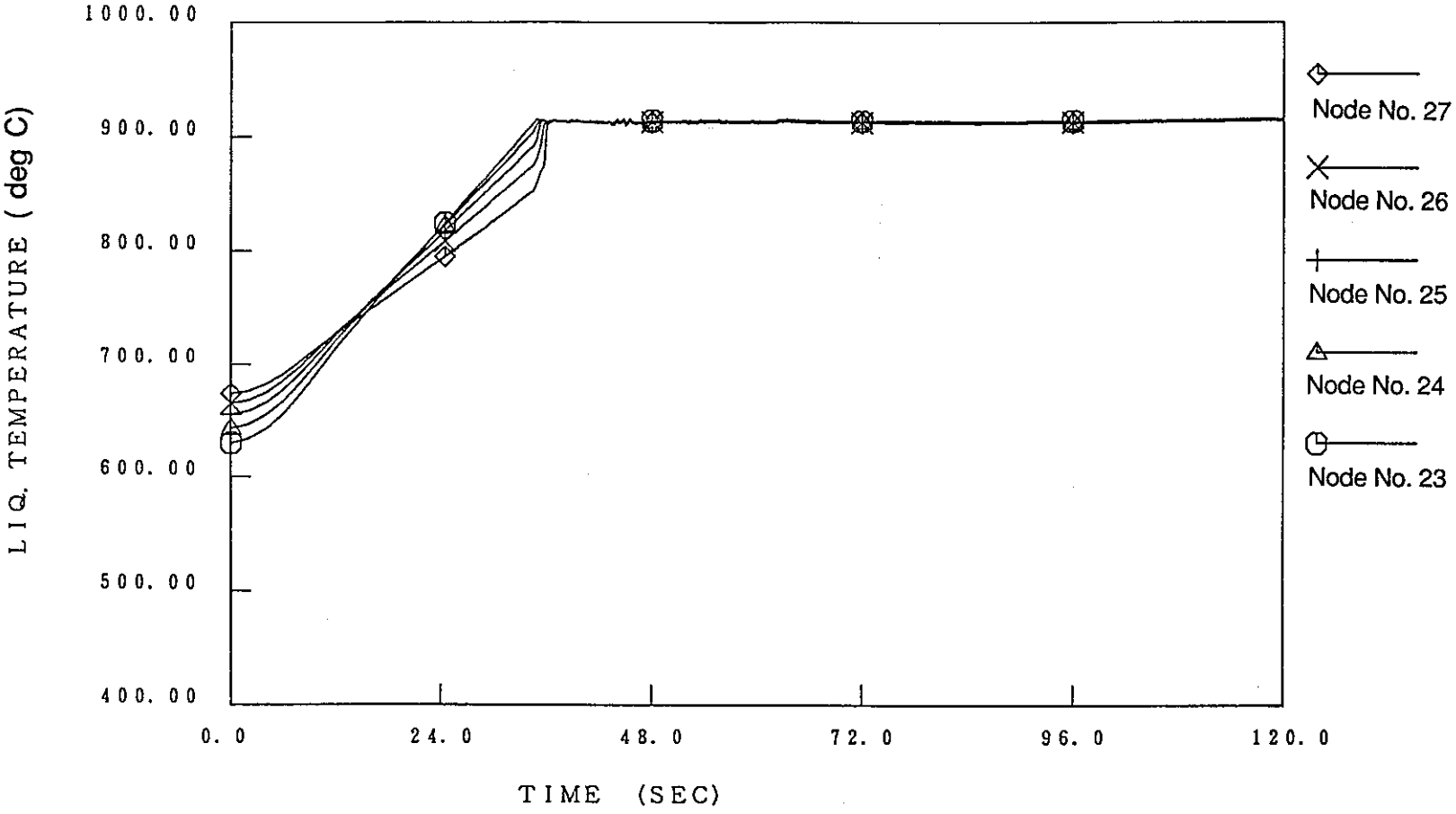

Figure 4.2 Calculated coolant temperature vs time curve.

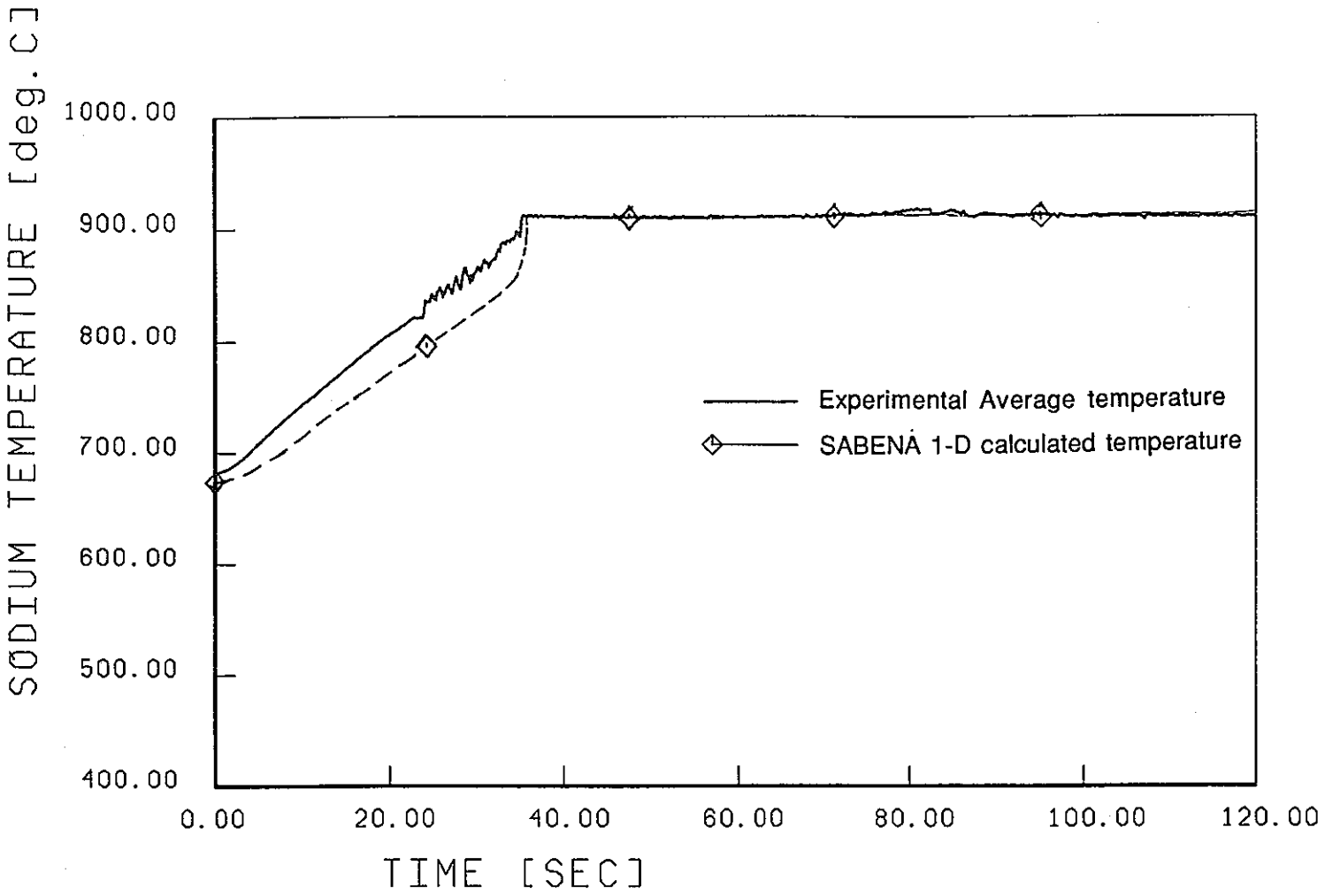

Figure 4.3 Sodium temperature time history curve (experimental average & calculated) at the top of heated section.

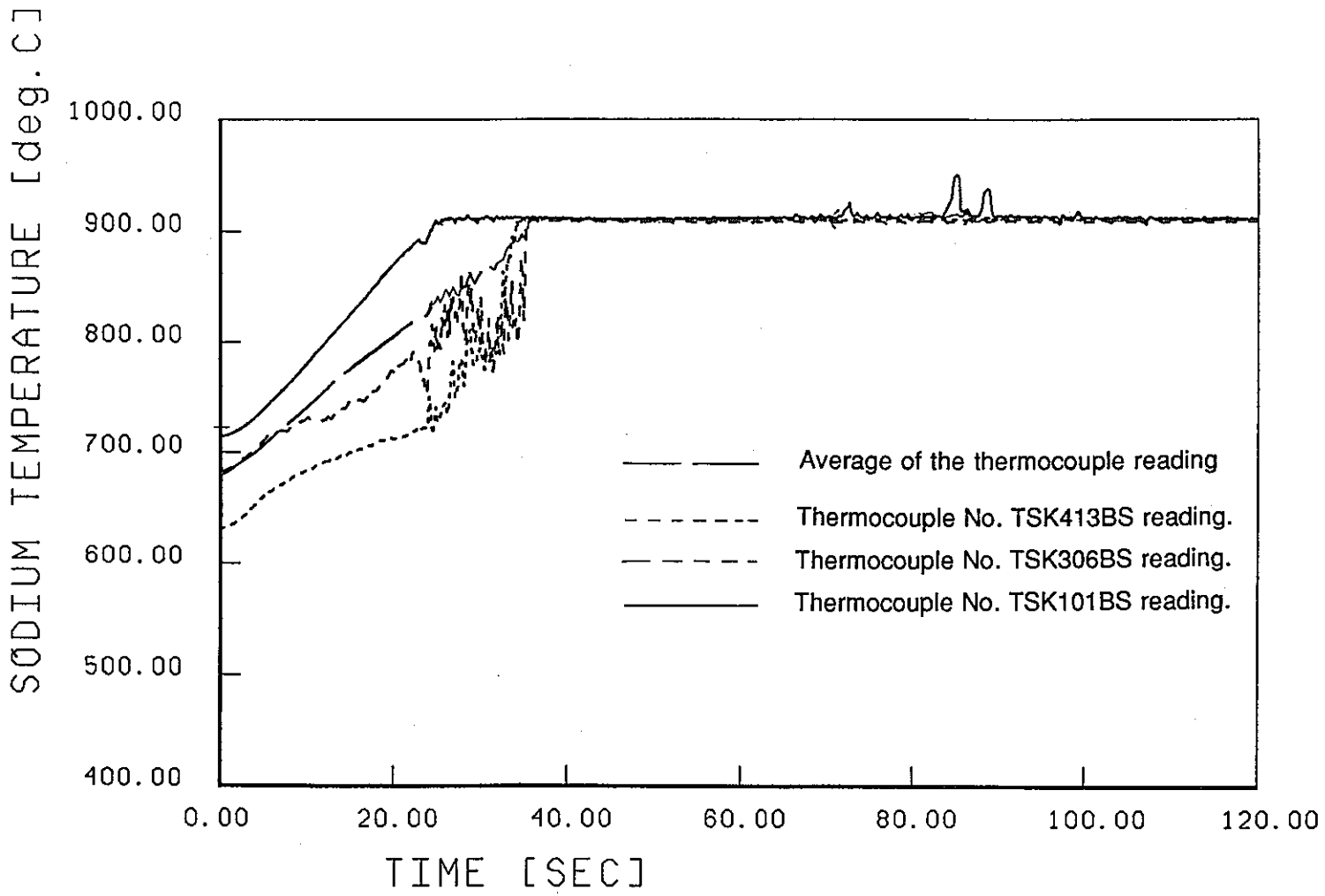

Figure 4.4 Sodium temperature at different radial position of the top of heated section & avg. calculated temperature vs. time curve.

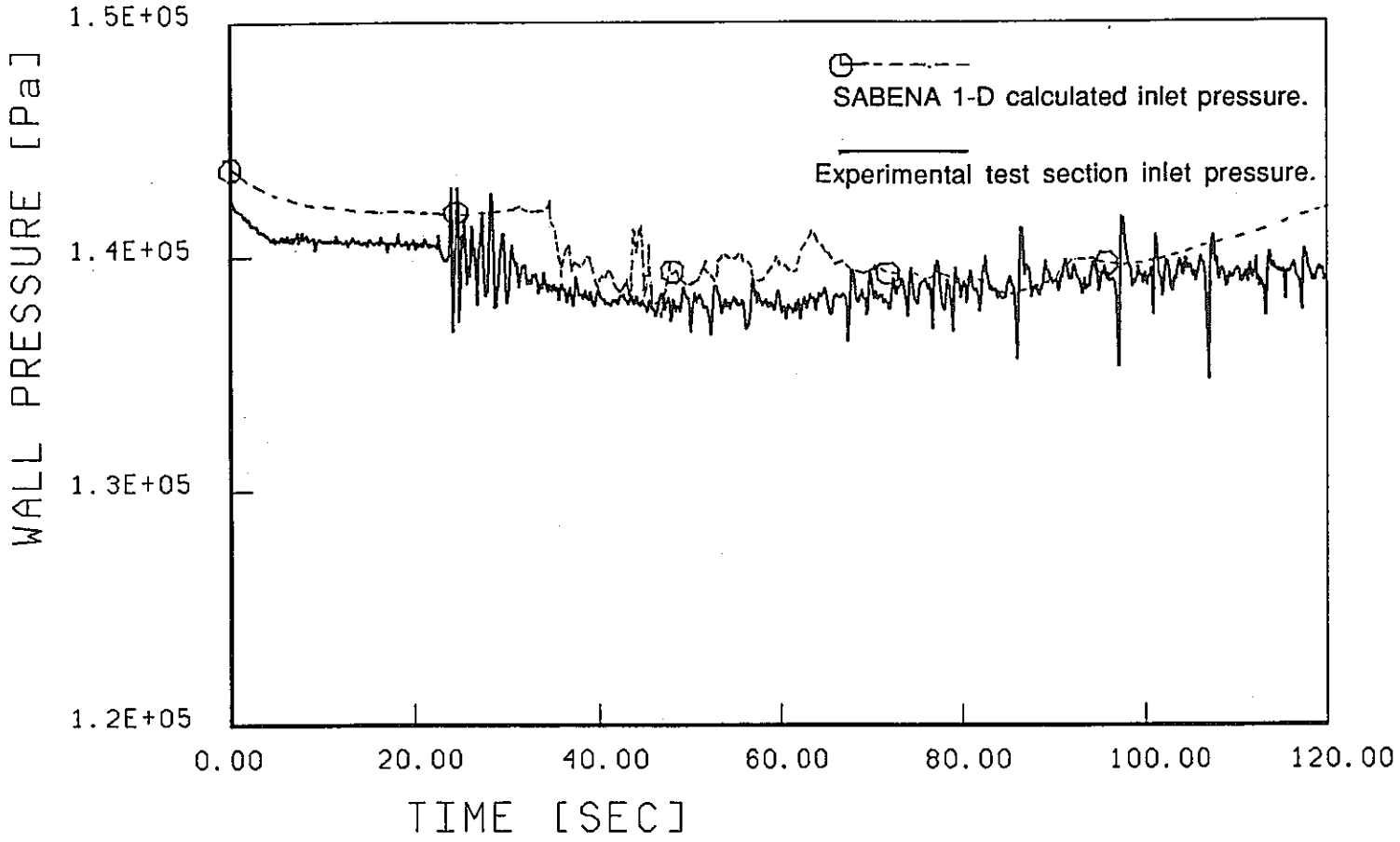

Figure 4.5 Inlet pressure vs. transient time curve

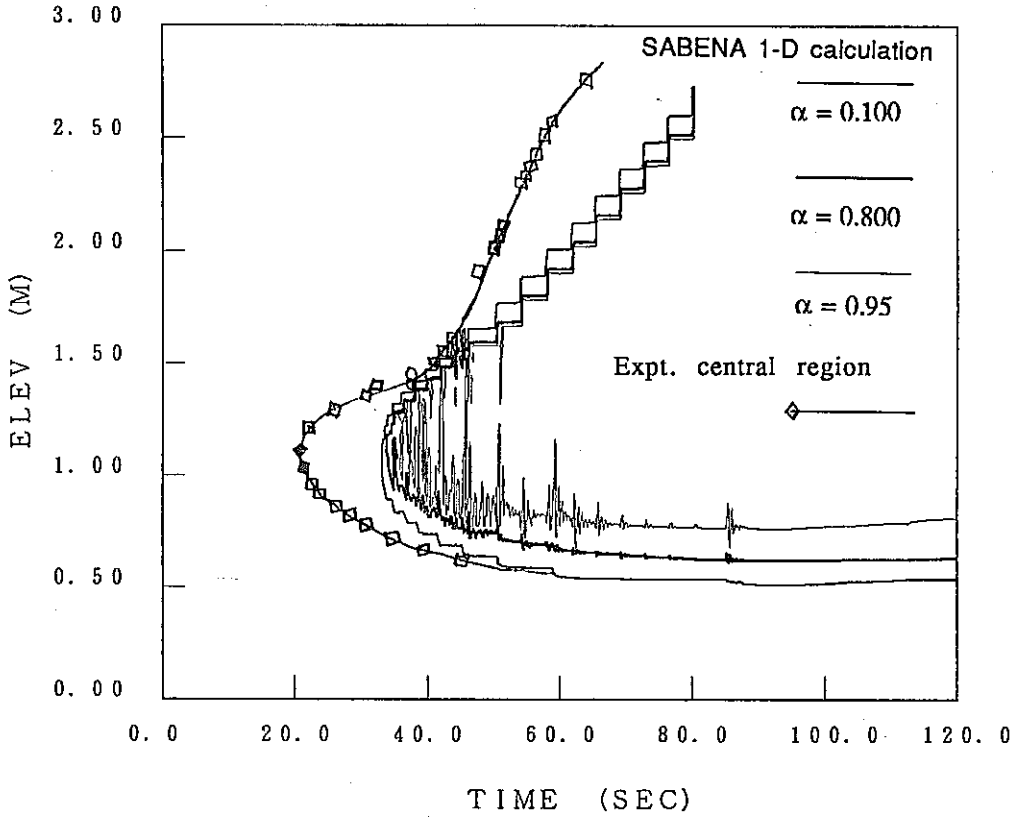

Figure 4.6 Calculated and experimental void progression curve.

5.Conclusion :

From the analysis we found that sodium, after the start of boiling, grew three dimensionally.

Our analysis of the experiment by Super System Code revealed that the homogeneous model can simulate the boiling phenomena quite accurately when the quality of boiling is low but at high quality boiling level the present model can not analyze the actual thermohydraulic phenomena. The incorporation of recent boiling correlations in SSC was found to be not good enough for accurate analysis. So, to predict the boiling phenomena at high quality level, more precise boiling correlations are needed to be formulated and to be used in SSC. Flow regime dependent correlations will probably give the best result.

The two-fluid two-phase separated flow model of SABENA 1-D was found to be accurate to simulate the low flow, low pressure high quality boiling phenomena. The axial voided region expansion inside the test channel both in the upstream region was also predicted accurately by the SABENA code. Average temperature calculation inside the heated section is also found to be in good agreement with the experimental average temperature.

So we can conclude that for high quality sodium boiling analysis, two-fluid two-phase separated flow model three dimensional analysis of the experiment will provide us with more accurate simulation of the experiment.

6. Appendix

A. Friedel correlation for frictional two-phase pressure gradient :

For $\mu_l/\mu_g <$ 1000, Friedel correlation is said to be the accurate available correlation for the frictional two-phase pressure gradient. It is written in terms of a two-phase multiplier

$$\phi_{lo}^2 = \left(\frac{-dp}{dz}\right)_F / \left(\frac{-dp}{dz}\right)_{lo}$$

where the numerator is the frictional pressure gradient in two-phase flow and the denominator is the frictional pressure gradient in single phase liquid flow with the same mass flow rate as the total two-phase flow rate. Then the correlation is given as

$$\phi_{lo}^2 = E + \frac{3.24FH}{Fr^{0.045}We^{0.035}}$$

$$E=(1-x)^2 + x^2\frac{\rho_l}{\rho_g}\frac{C_{fgo}}{C_{flo}}$$

$$F= x^{0.78}(1-x)^{0.224}$$

$$H = \left(\frac{\rho_l}{\rho_g}\right)^{0.91}\left(\frac{\mu_g}{\mu_l}\right)^{0.19}\left(1-\frac{\mu_g}{\mu_l}\right)^{0.7}$$

$$Fr = \frac{G^2}{gd\rho_h^2}$$

$$We = \frac{g^2 d}{\sigma\rho_h}$$

and

$$\rho_h = \left(\frac{x}{\rho_g} + \frac{1-x}{\rho_l}\right)^{-1}$$

Where x is the quality, ρ_g is the gas density, ρ_l is the liquid density, C_{fgo} & C_{flo} are the friction factor for the total mass flux flowing with the gas and liquid properties respectively, μ_g & μ_l are the gas and liquid viscosity respectively, σ is the surface tension and g is the acceleration due to gravity.

The above correlation is applicable to vertical upflow and to horizontal flow.

Figure 5.1 shows the two-phase friction multiplier value at different qulity for the Friedel and SSC's friction model. It is to noted here that Friedel result depends on the mass flux and the following curve corresponds to LOF-15057's mass flux value at the beginning of the boiling.

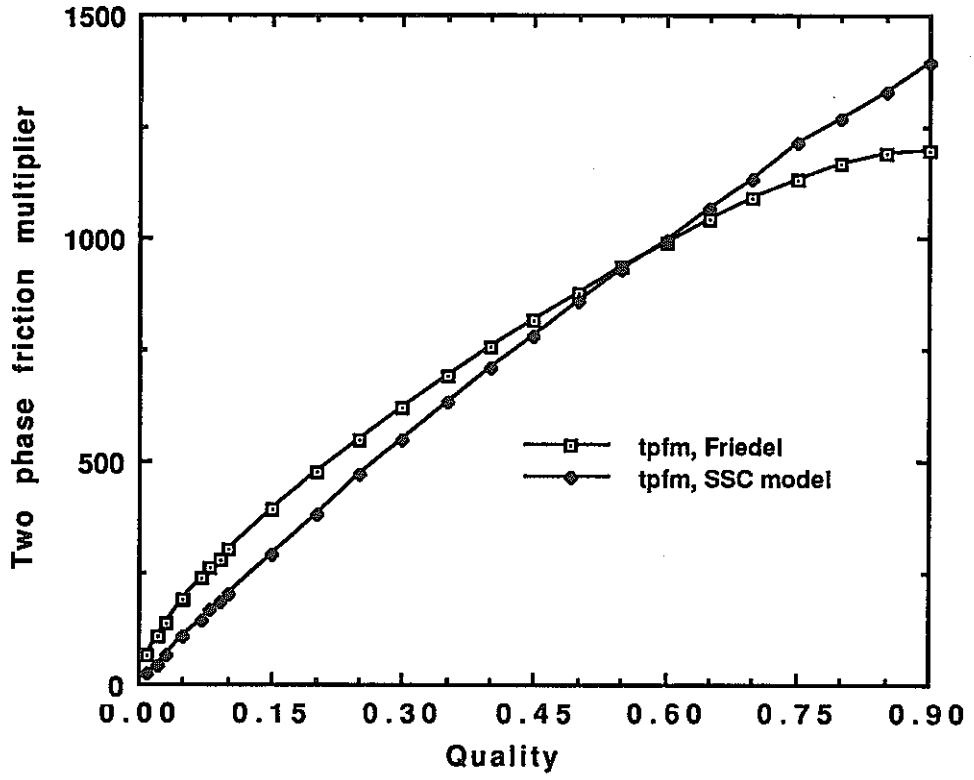

Figure:5.1 Comparison between Friedel & SSC's friction multiplier model

B. CISE correlation for void fraction determination :

The correlation of Premoli et al., usually known as the CISE correlation is a correlation in terms of the slip ratio S. The void fraction is then given by

$$\alpha = \frac{1}{1+\left(S\frac{1-x}{x}\frac{\rho_g}{\rho_l}\right)}$$

The slip ratio is then given by

$$S = 1 + E_1\left(\frac{y}{1+yE_2} - yE_2\right)^{0.5}$$

Where

$$y = \frac{\beta}{1-\beta}$$

$$\beta = \frac{\rho_l x}{\rho_l x + \rho_g(1-x)}$$

$$E_1 = 1.578\ Re^{-0.19}\left(\frac{\rho_l}{\rho_g}\right)^{0.22}$$

$$E_2 = 0.0273\ We\ Re^{-0.51}\left(\frac{\rho_l}{\rho_g}\right)^{-0.08}$$

$$Re = \frac{Gd}{\mu_l}$$

and

$$We = \frac{G^2 d}{\sigma \rho_l}$$

where x is the quality, ρ_l & ρ_g are the liquid and gas density, μ_l & μ_g are the liquid and gas viscosity, G is the total mass flux and σ is the surface tension.

Figure 5.2 in the following page shows the void fraction values at different quality for the CISE and Lockhart-Martinelli correlation. CISE void fraction value depends on mass flux value and the following CISE curve is based on the PLANDTL LOF - 15057 experiment's mass flux value at the start of boiling.

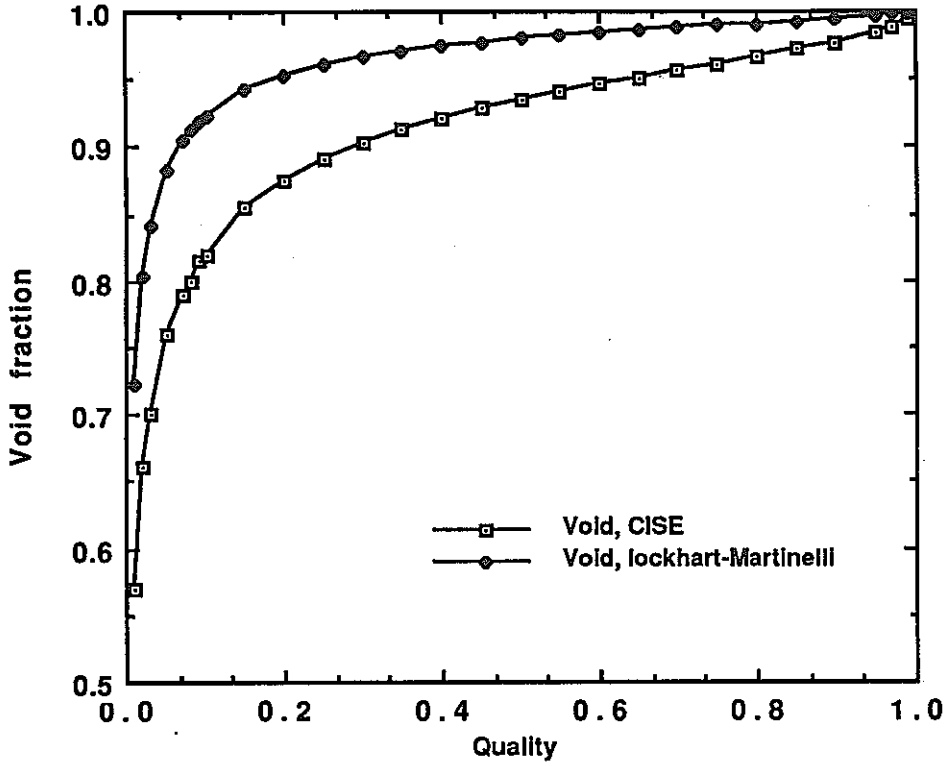

Figure 5.2 Comparison between CISE & Lockhart-Martinelli void fraction model

7. References

1. M. Ishii and K. Mishima, Two-fluid model and hydrodynamic constitutive relations, Nuclear Engineering and Design, 82(1984)107.

2. A. L. Scwor, M. S. Kazimi and N. E. Todreas, Advances in two-phase flow modelling for LMFBR application, Nuclear Engineering and design, 82(1984)127.

3. G. Hestroni, Hand book of multiphase systems, (McGrawHill Book Company.)

4. P. V. Whalley, Boiling, condensation and gas Liquid flow, (Clarendon Press, Oxford, 1987)

5. H. Ninokata, K. Baba and T. Okano, SABENA : Two-fluid model computer programme for the sodium boiling analysis of LMFBR system.

6. J. G. Guppy, Super System Code (SSC Rev.2), An advanced thermohydraulic simulation code for transient in LMFBRs, NUREG/CR-3169, April1983.

7. F. Huber, A. Kaiser, et al., Steady state and transient sodium boiling experiments in a 37 pin bundle, Nuclear Engineering and Design, 100(1987) 377.

8. A. Kaiser and W. Peppler, Sodium boiling experiment in a seven pin bundle : flow patterns and two-phase pressure drop, Nuclear Engineering Design, 43(1977)285.

9. M. K. Rahbar & Erik. G. Cazzoli, Modelling and analysis of low heat flux natural convection sodium boiling in LMFBR, report, Brookhaven National Laboratory,USA.